

TNO report

Delft Cluster – Bijzondere Belastingen

Full system response Thomassen tunnel under impact load using LS-DYNA (concept version 3)

Date 4 December 2009

Author(s) ir. H.G. Burggraaf
dr. ir. A.H.J.M. Vervuurt
dr. ir. J. Weerheijm

Assignor

Project number 034. 77264/01.01

Classification report

Title

Abstract

Report text

Appendices

Number of pages 46 (incl. appendices)

Number of appendices

All rights reserved. No part of this report may be reproduced and/or published in any form by print, photoprint, microfilm or any other means without the previous written permission from TNO.

All information which is classified according to Dutch regulations shall be treated by the recipient in the same way as classified information of corresponding value in his own country. No part of this information will be disclosed to any third party.

In case this report was drafted on instructions, the rights and obligations of contracting parties are subject to either the Standard Conditions for Research Instructions given to TNO, or the relevant agreement concluded between the contracting parties. Submitting the report for inspection to parties who have a direct interest is permitted.

Contents

1	Introduction.....	3
1.1	Background of the project.....	3
1.2	Project description	3
1.3	Work package R3.....	4
1.4	Scope of this report.....	4
2	Analysis model description.....	5
2.1	Introduction.....	5
2.2	Geometry Thomassen tunnel	6
2.3	Used mesh and boundary conditions	7
2.4	Material properties	8
2.5	Loading	9
3	Analysis results reduced BLEVE	11
3.1	Introduction.....	11
3.2	Tunnel displacements	11
3.3	Concrete damage and strains	14
3.4	Reinforcement stresses	20
3.5	Soil displacements, displacements, velocities and accelerations	23
4	Analysis results maximum BLEVE.....	27
4.1	Introduction.....	27
4.2	Tunnel displacements	27
4.3	Concrete damage and strains	30
4.4	Reinforcement stresses and strains	35
4.5	Soil displacements, displacements, velocities and accelerations	40
5	Comparison results LS-DYNA and PLAXIS	44
6	Conclusions and recommendations	45
	References.....	46

1 Introduction

1.1 Background of the project

In the Netherlands the available land is used more and more intensively. Main corridors of transport (roads and railroads) are part of the urban area. In order to avoid the negative influences of the corridors of transport (noise, pollution, barriers for local transport) many main corridors of transport will be built in tunnels. The responsible authorities have to decide whether dangerous goods may be transported through these tunnels. First, their attention focuses on the safety of human beings in the tunnel. However, also the integrity of the structure and the economic consequences of an accident must be considered. For the last aspect, knowledge of the loading mechanism and the structural response is required.

Nowadays the goods which are sensitive for explosion are transported along alternative routes that exclude tunnels. These are mostly secondary roads. The transport along these alternative roads has many disadvantages, such as the safety along the route, the air- and noise pollution along the road and the higher transport costs. Therefore, it is preferred to permit the transport of dangerous goods through tunnels. In case of multiple use of space this leads to the question what are the possible consequences and risks for buildings of structures above the tunnel.

In the Delft Cluster work package “Bijzondere Belastingen” (CT01.21) the consequences of a BLEVE¹ and a reduced BLEVE are considered. These phenomena have a low probability of occurrence, but might have immense consequences. Therefore, a deterministic consideration seems not possible.

The results of the work package must facilitate the quantitative risk analysis of the phenomena, that support the authorities in their decision of allowing transport of dangerous goods through tunnels or not. The work package focus is on the mechanical description of the loading and the response. However, it requires an interdisciplinary approach, which integrates knowledge of risk analysis, explosion and evaporation of liquefied gases, structural dynamics and soil dynamics.

1.2 Project description

The project contains two main stream research lines:

1. Loading due to BLEVE. The BLEVE research is mainly executed in a PhD project at Delft University of Technology. This part focuses on an improved understanding and modelling of the BLEVE phenomenon. TNO Defense and Safety will participate in this research line by introduction of practical mechanical modelling of the vessel behaviour and creation of a practical engineering model for BLEVE load prediction, based on the results of a PhD-study.

¹ BLEVE (Boiling Liquid Expanding Vapor Explosion) is the phenomenon of an extremely fast evaporation of liquefied gas that occurs after the containing vessel has failed. Blast waves are generated which are comparable to the blast of an explosion.

2. Dynamic Response of the structure-soil system under BLEVE and a reduced BLEVE loading. Here TNO Built Environment and Geosciences concentrates on the structural part of the problem, whereas Deltares and Delft University of Technology will take care of the soil response. TNO Defense and Safety will provide data on appropriate loads for realistic cases.

The project is divided into the following work packages:

- L1: Mechanical aspects of the initiation of a BLEVE
- L2: Thermodynamic and gas dynamic aspects of a BLEVE
- R1: Preliminary structural response
- R2: Soil behaviour
- R3: Full system response
- R4: Consequences for surroundings

This report is part of work package R3.

1.3 Work package R3

Work package R3 of the Delft Cluster project 'Bijzondere Belastingen' aims at the 'full system response' of tunnels under the influence of an explosion load. In this work package finite element calculations were performed, where the Thomassen tunnel was elected as a benchmark. Besides the response of the tunnel structure, also the response of the surrounding soil was considered.

The study was conducted by TNO and Deltares. Deltares has studied the dynamic behaviour of the soil. The dynamic properties of the soil were used by TNO to model the entire system of the tunnel and the surrounding soil. The calculations of TNO were performed with the finite element program LS-DYNA, with an advanced material model for the tunnel and a simple material model to the surrounding soil. The calculations of Deltares were performed with the finite element program PLAXIS, with a simple material model for the tunnel and an advanced material model for the land. This approach was chosen because there are no programs available with good, advanced material models for both the tunnel structure and the surrounding soil.

The purpose of the work package R3 is to obtain clarity on the possibilities to quantify the overall response of the tunnel system (tunnel lining and surrounding soil) using (advanced) numeric codes. Derived goals are obtaining clarity on the role of soil in the response to the explosion load and preparing a draft methodology for assessing explosion-proof tunnels.

1.4 Scope of this report

This report describes the research on the dynamic response and failure of the Thomassen tunnel (formerly known as the Caland tunnel) under a blast explosion. A full dynamic analysis is done using the explicit finite element code LS-DYNA. Chapter 2 gives a description of the finite element model. The results of the calculations are presented in chapter 3. Finally, some conclusions and recommendations are given in chapter 4.

2 Analysis model description

2.1 Introduction

The dynamic behavior of the Thomassen Tunnel under the influence of a BLEVE load was previously investigated using the finite element program DIANA and LS-DYNA, see [1]. This previous research revealed that DIANA and LS-DYNA are suitable platforms for the modeling of high impact loading of structures, but implementation of time-dependent reaction (strain rate dependency) is less ambiguous in DIANA than in LS-DYNA. In addition, the program structure and the solution methodology (explicit solver) of LS-DYNA are more suitable for dynamic calculations than the program structure and solution method (implicit solver) of DIANA. For this reason, in the present study LS-DYNA was used.

Previous calculations with LS-DYNA, see [2], on a tunnel without surrounding soil have indicated that a BLEVE-load (maximum pressure 510 kPa, pulse 12 kPa·s) gives local damage in the middle wall of the tunnel. Yielding of the reinforcement did not occur. On this basis, it was concluded that no global collapse occurs. As noted, the surrounding soil was not included in this study. Since there are no programs available with good, advanced material models for both the tunnel structure and the surrounding soil, both LS-DYNA and PLAXIS are used to quantify the full system response. In PLAXIS a relatively simple model for the tunnel is used. In LS-DYNA a simplified soil model is used. Finally the results are compared.

The calculations in LS-DYNA focus on the initial respons. Long-term issues such as rebound effects and the stability of the overall tunnel structure have not been studied. The calculations are based on a conservative maximum BLEVE-load and a reduced BLEVE-load. The reduction is based on research of the BLEVE mechanism, see [3].

To predict the dynamic behaviour of the tunnel, both the inertia and stiffness of the surrounding soil are considered in the calculations. The water above the tunnel is modelled as a uniformly distributed load on the tunnel. The inertia of the water is not included in the calculations. Unpublished results show that the inertia of the water does not affect the results significantly.

The influence of the soil on the full system response is studied by a sensitivity study in LS-DYNA. The following situations are considered (G = shear modulus, Δp = pressure difference, I = pulse):

1. Soft soil ($G = 5$ MPa) and a reduced BLEVE-load ($\Delta p = 510$ kPa; $I = 12$ kPa·s);
2. Stiff soil ($G = 150$ MPa) and a reduced BLEVE-load ($\Delta p = 510$ kPa; $I = 12$ kPa·s);
3. Soft soil ($G = 5$ MPa) and a maximum BLEVE-load ($\Delta p = 1600$ kPa; $I = 64$ kPa·s);
4. Stiff soil ($G = 150$ MPa) and a maximum BLEVE-load ($\Delta p = 1600$ kPa; $I = 64$ kPa·s).

In this chapter the tunnel geometry is outlined in section 2.2. The used mesh and the boundary conditions are presented in section 2.3. The material properties are given in section 2.4. Finally the loading is discussed in section 2.5.

2.2 Geometry Thomassen tunnel

An overview of the geometry of the Thomassen tunnel is given in figure 2.1.

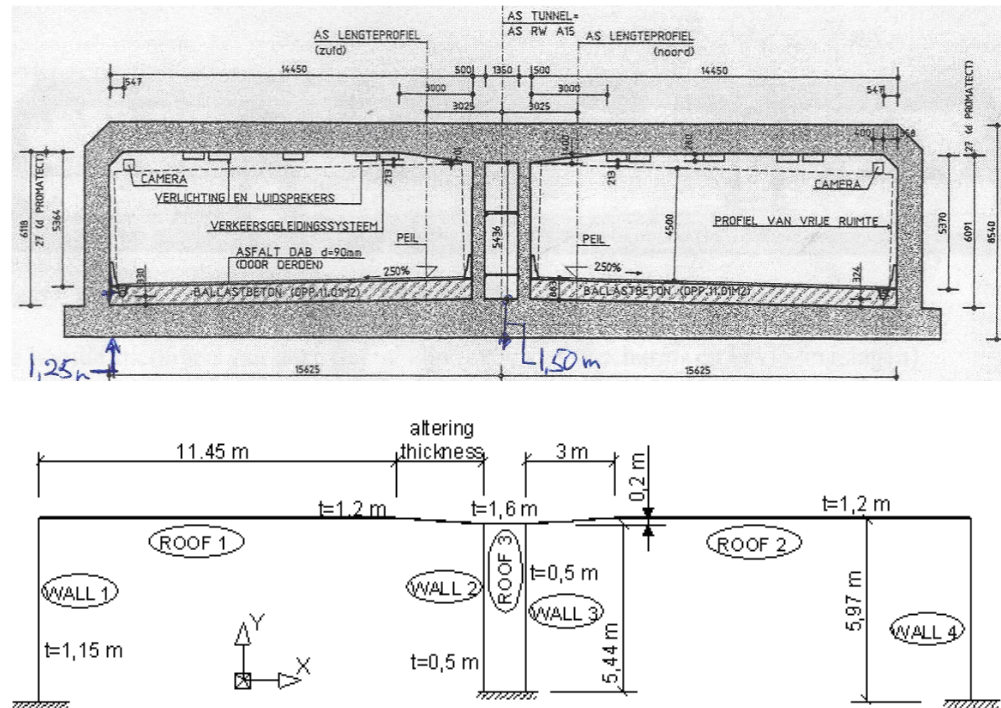


Figure 2.1: Geometry of the Thomassen tunnel

The reinforcement is given in Figure 2.2. In this figure the group names of the different reinforcement sections are given, as well as the location of the rebars. The geometry (cross sectional areas, length) and the concrete cover to the rebars are given in table 2.1. Shear reinforcement is not taken into account.

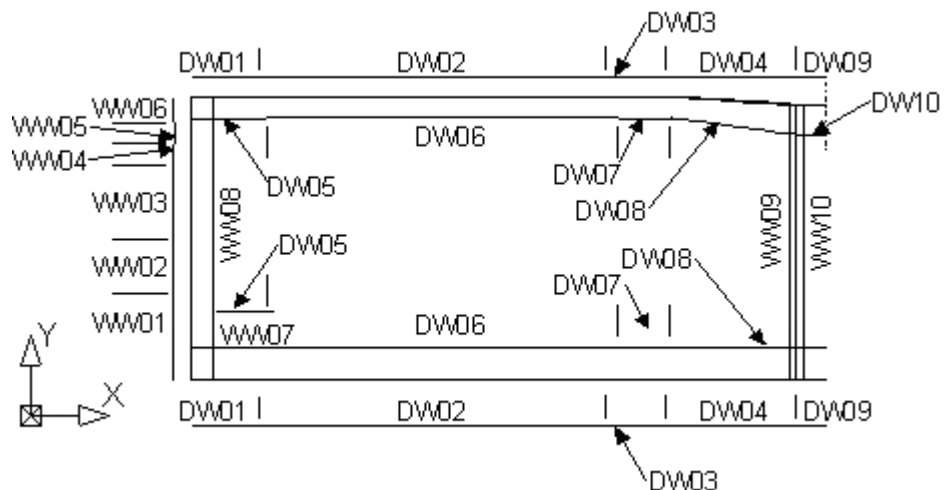


Figure 2.2: Group names of the reinforcement in the FE-model

Table 2.1: Reinforcement properties: A_s represents the cross sectional area and c' is the concrete cover from the gravity centre of the rebars

Name	A_s (mm ² /m)	c' (mm)	Length (m)
Walls			
WW01	1340 ^{*)}	62	1.3
WW02	2094	81	1.3
WW03	1047	91	1.8
WW04	2094	91	0.5
WW05	3727	123	0.5
WW06	4774	113	0.6
WW07	7454	123	1.3
WW08	8500	134	5.3
WW09	11180	153	full height
WW10	8500	134	full height
Roof/ Floor			
DW01	7454	143	1.6
DW02	2094	96	8.35
DW03	5360	102	1.4
DW04	13400	131	3.1
DW05	2094	65	2.4
DW06	7454	112	8.4
DW07	2094	65	1.25
DW08	2094	65	3.0
Rescue tube			
DW09	13400	65	1.35 (full roof width)
DW10	2094	131	1.35 (full roof width)

^{*)} excluding crossing reinforcement from the floor of the tunnel

2.3 Used mesh and boundary conditions

A 0,1 m thick section of the tunnel and the surrounding soil is modelled with two layers of solids in the thickness (z) direction. In between the rebars are modelled with beam elements. Complete adhesion between rebars and solids is assumed. The mesh is shown in figure 2.3. The rebars are shown in figure 2.4.

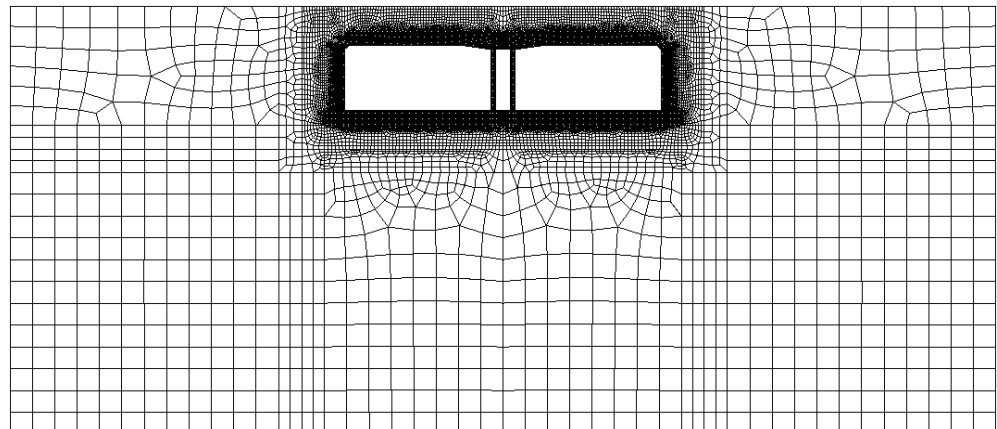


Figure 2.3: Solid mesh

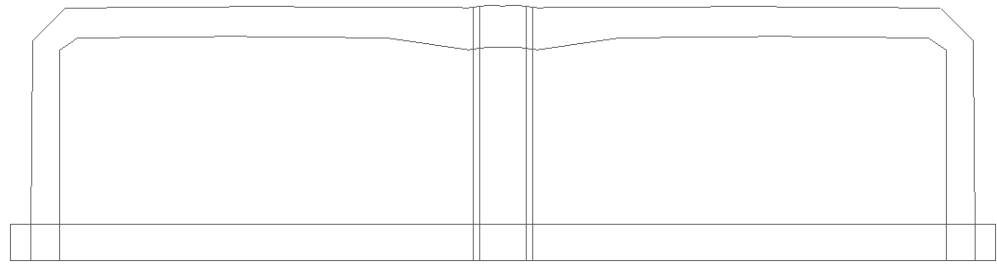


Figure 2.4: Rebars

To simulate a plain strain state, displacements in the out of plane direction are prevented. Non reflecting boundaries are used along the perimeter to avoid spurious reflections. For the lower boundary the vertical displacements are set to zero. For the side boundaries the horizontal displacements are set to zero.

2.4 Material properties

In the analyses the concrete behaviour is modelled using the material model *MAT_Concrete_Damage_Rel3. This model generates the material parameters based on the compressive strength, which is set to 35 MPa. Strain rate hardening of concrete in tension and compression is accounted for, using data from literature. The concrete behaviour is shown schematically in figure 2.5. The material properties for are summarised in table 2.2.

The reinforcement behaviour is modelled using the Von-Mises plasticity model *MAT_PLASTIC_KINEMATIC with strain and strain rate hardening. The material properties are summarised in table 2.3.

Finally the soil behaviour is modelled using the Mohr-Coulomb model *MAT_MOHR_COULOMB. The material properties are summarised in table 2.4.

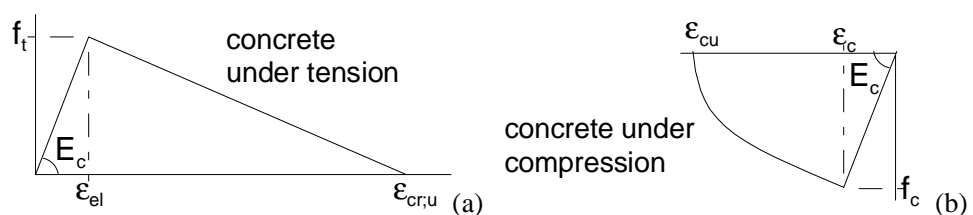


Figure 2.5: Material model for concrete under tension (a) and compression (b)

Table 2.2: Material properties concrete (concrete strength class B35)

Property	Value
Young's modulus	$E_c = 26500 \text{ N/mm}^2$
compressive strength	$f_c = 35 \text{ N/mm}^2$
compressive failure strain	$\epsilon_{cu} = 3,5 \text{ ‰}$
tensile strength	$f_t = 3,22 \text{ N/mm}^2$
tensile failure strain	$\epsilon_{cr,u} = 2,05 \text{ ‰}$
mass	$\rho = 2400 \text{ kg/m}^3$

Table 2.3: Material properties reinforcement (steel FeB500)

Property	Value
Young's modulus	$E_s = 200000 \text{ N/mm}^2$
strength	$f_s = 530 \text{ N/mm}^2$
failure strain	$\epsilon_{su} = 3,25 \%$
contraction coefficient	$\nu = 0,3$
mass	$\rho = 7850 \text{ kg/m}^3$

Table 2.4: Material properties soil

Property	Value
shear modulus	$G = 5 \text{ N/mm}^2$ (soft soil) / $G = 150 \text{ N/mm}^2$ (stiff soil)
cohesion	1 kPa
angle of friction	30°
angle of dilatation	0°
contraction coefficient	$\nu = 0,48$
mass	$\rho = 2000 \text{ kg/m}^3$

2.5 Loading

The loads are applied in two steps:

1. Static load (self weight, soil and water pressure). To avoid dynamic effects, the static load is applied slowly using a ramp function between $t = 0$ and 0,2 sec. This is done in combination with critical damping.
2. Blast load. The blast load is applied at $t = 0,2$ sec, until the end of the analysis, without damping.

The static and blast load are shown in figure 2.6.

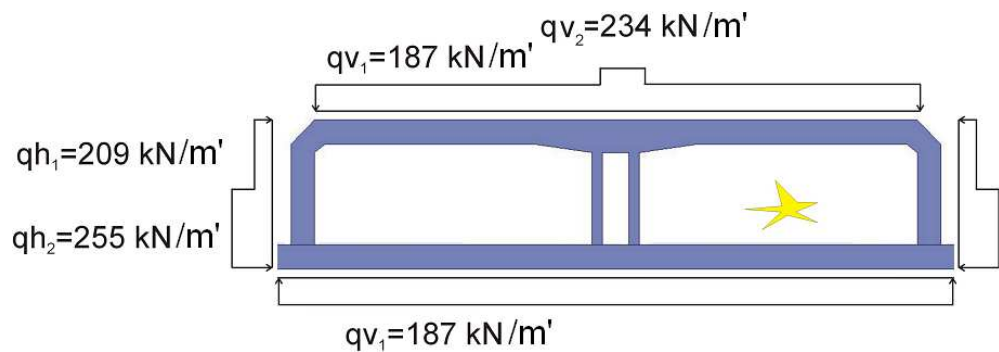


Figure 2.6: Static and blast load

For the blast loading a reduced and a maximum BLEVE-load is used. The numerical data are given in table 2.5 and 2.6. A graph of the load as function of time is shown in figure 2.7 and 2.8.

Table 2.5: Reduced BLEVE-load

Time [s]	Pressure [kPa]
0	0
0.00001	513
0.02	130
0.08	30
0.15	0

Table 2.6: Maximum BLEVE-load

Time [s]	Pressure [kPa]
0	0
0.00001	1617
0.0328	410
0.1312	95
0.246	0

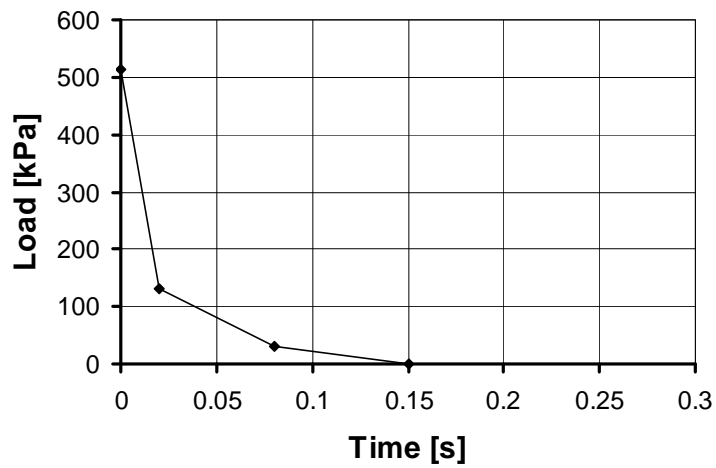


Figure 2.7: Reduced BLEVE-load

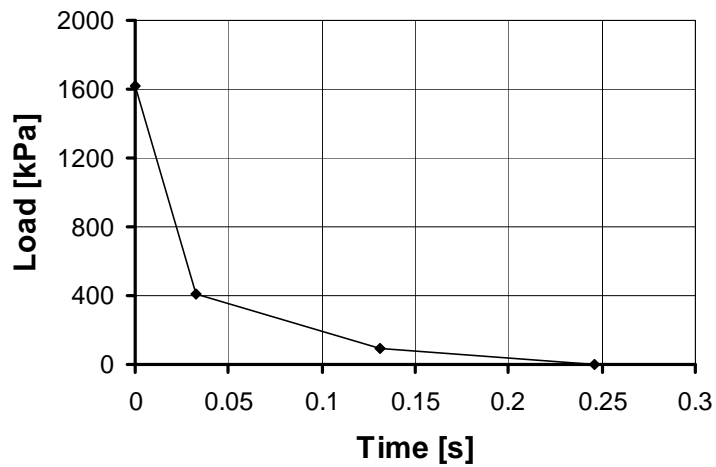


Figure 2.8: Maximum BLEVE-load

3 Analysis results reduced BLEVE

3.1 Introduction

In this chapter the results of the finite element analyses for a reduced BLEVE-load are presented. First, in section 3.2 the displacements of the tunnel are discussed. In section 3.3 the concrete damage and strains are given. In section 3.4 the reinforcement stresses are presented. Finally, in section 3.5 the soil stresses, displacements, velocities and accelerations are given.

3.2 Tunnel displacements

Figure 3.1 shows the nodes in the roof and floor that have been used for analysing the vertical displacements. Figure 3.2 shows the nodes in the walls that have been used for analysing the horizontal displacements.

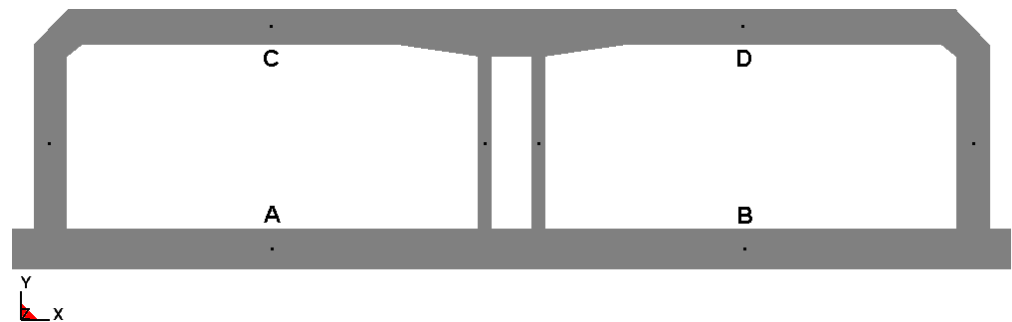


Figure 3.1: Nodes used for analysing the vertical displacements

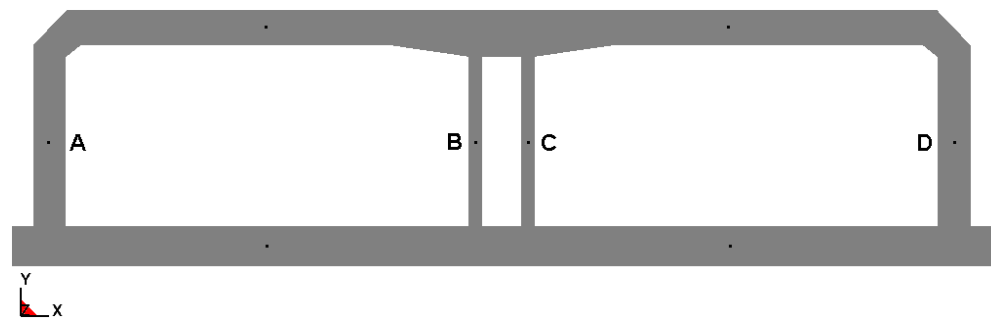


Figure 3.2: Nodes used for analysing the horizontal displacements

The vertical displacement histories of the roof and the floor are presented in figure 3.3 and 3.4 for respectively soft and stiff soil. The horizontal displacement histories of the walls are presented in figure 3.5 and 3.6. Observe that the influence of the stiffness of the soil is marginal for the behaviour of the tunnel and that the soil properties are not relevant, within the prescribed limits ($5 \leq G \leq 150$ MPa) for the soil stiffness. In case of liquefaction of the soil, it is possible that the influence of the soil is larger for the stability and eventual damage to the tunnel.

The maximum vertical static displacement (due to self-weight and soil and water pressure) for the roof and the floor is 5 mm. When the reduced BLEVE-load is introduced, the roof of the right tunnel tube (where the explosion is present) will move upwards and the floor will move downwards. For the left tunnel tube there's an opposite response. The maximum vertical displacement for the roof and the floor during the reduced BLEVE-load is about 10 mm. This is a doubling of the static displacement. Furthermore after 1 sec an equilibrium occurs, where damage in the roof and (to a lesser extent) in the floor leads to a permanent displacement of the roof and the floor.

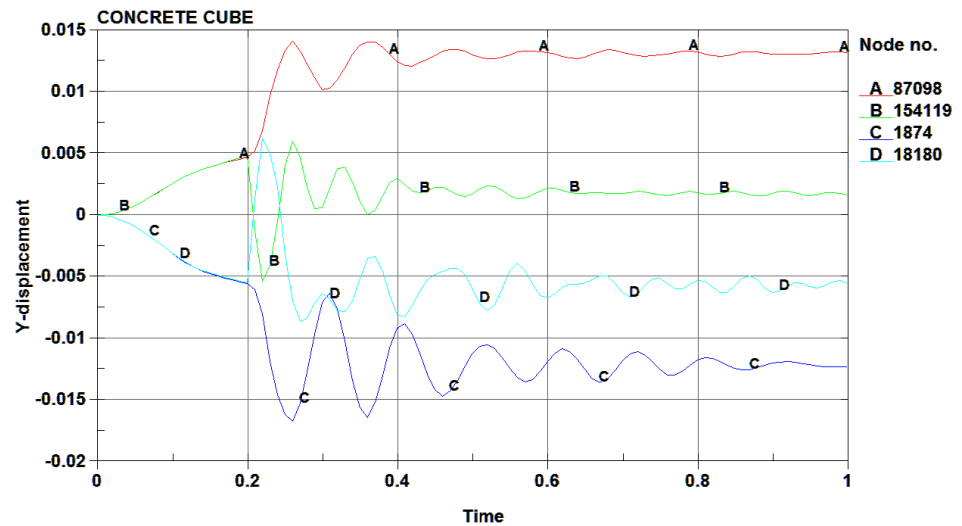


Figure 3.3: Vertical displacements of roof and floor in soft soil for a reduced BLEVE

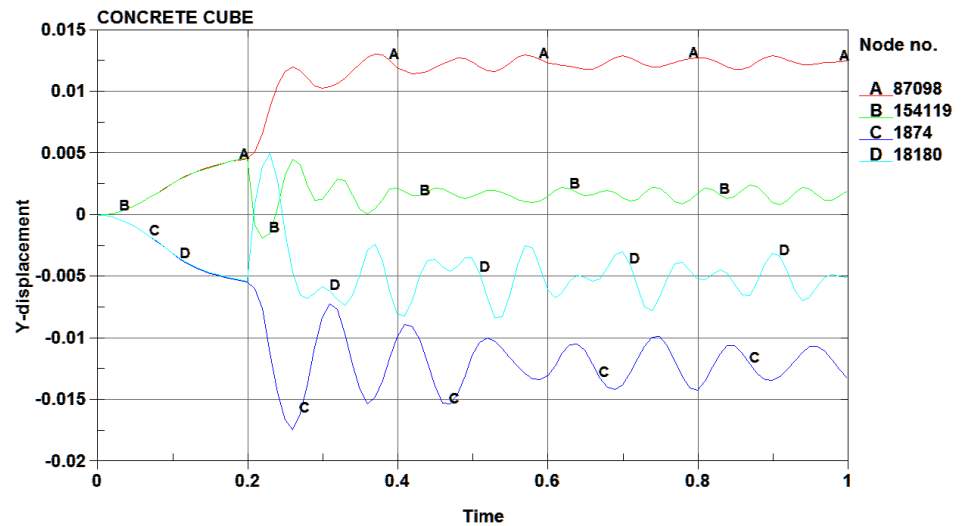


Figure 3.4: Vertical displacements of roof and floor in stiff soil for a reduced BLEVE

The horizontal static displacements of the walls are approximately 1 mm. After applying the reduced BLEVE-load, the inner wall in the right tube will move in direction of the escape tube. The maximum horizontal displacement of this wall is reached after 0,1 sec and is approximately 150 mm. The horizontal displacements of the other walls are relatively small (approximately 5 mm).

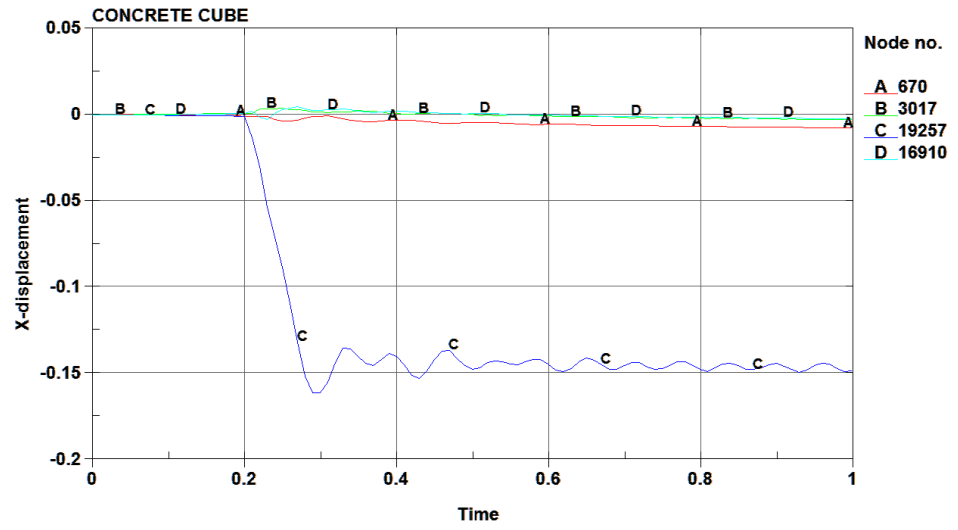


Figure 3.5: Horizontal displacements of walls in soft soil for a reduced BLEVE

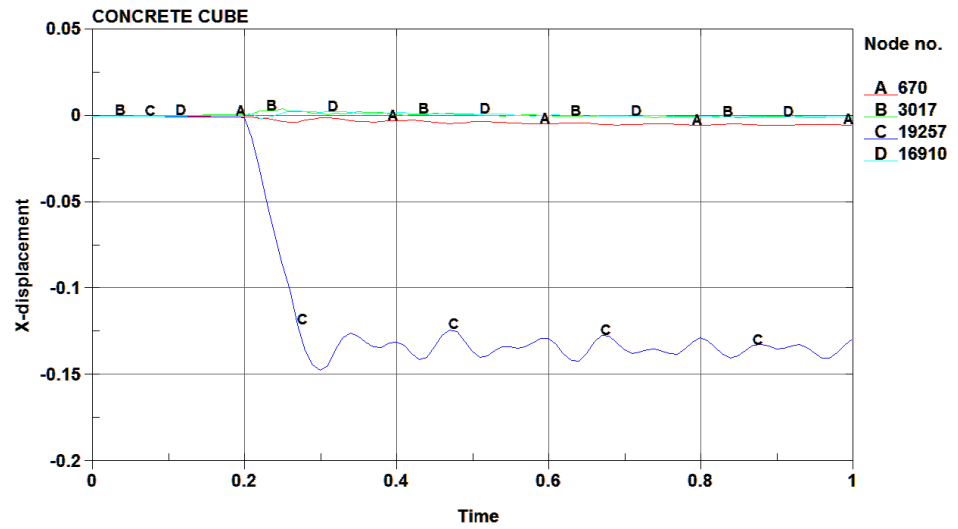


Figure 3.6: Horizontal displacements of walls in stiff soil for a reduced BLEVE

3.3 Concrete damage and strains

The MAT_72R3 concrete material defines damage by means of a scalar parameter which ranges between 0 (undamaged) and 2 (damaged). Damage occurs under compression (plasticity) and under tension (crack formation). The behaviour of the reinforcement has no effect on the damage parameter. It is further noted that the damage is not reversible (once damaged, remains damaged), despite the fact that in case of cyclic loads the concrete behaviour is reversible.

The damage caused by the permanent load is shown in figure 3.7. The permanent load causes some cracking in the roof and the floor, under and above the inner walls. There's also some cracking in the midspan zones and at the connection between the roof and the outer walls.

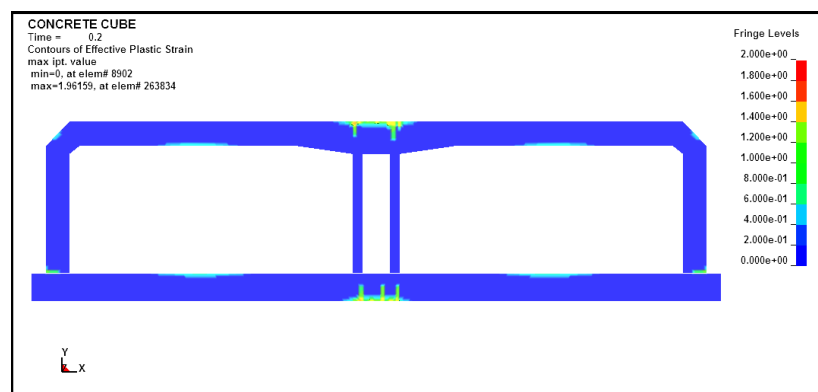


Figure 3.7: Damage due to self-weight and soil and water pressure

The evolution of the damage is shown in figure 3.8 and 3.9 respectively for soft and stiff soil. In the first response, the effect of the blast load is opposite to the permanent load, causing bending of the roof in upward direction and bending of the floor in downward direction. In the left tunnel tube the blast and the permanent load work in same direction, thus increasing the bending downwards for the roof and increasing the bending upwards for the floor.

The most critical part is the inner wall of the right tunnel tube. Already 0,03 sec after the start of the blast, this wall is fully damaged. Because the blast load is still present then, there's a possibility that parts of this wall will hit the other inner wall, which may lead to failure of the other inner wall too. The finite element analyses don't account for this phenomenon.

Because the tunnel is modelled in 2D, it is unknown over which length in longitudinal direction the damage in the inner wall will occur. It is expected that the damage will lead to a local collapse of the inner wall, but will not lead to a global collapse of the tunnel lining. More research, for example with 3D-models, is needed to verify this expectation.

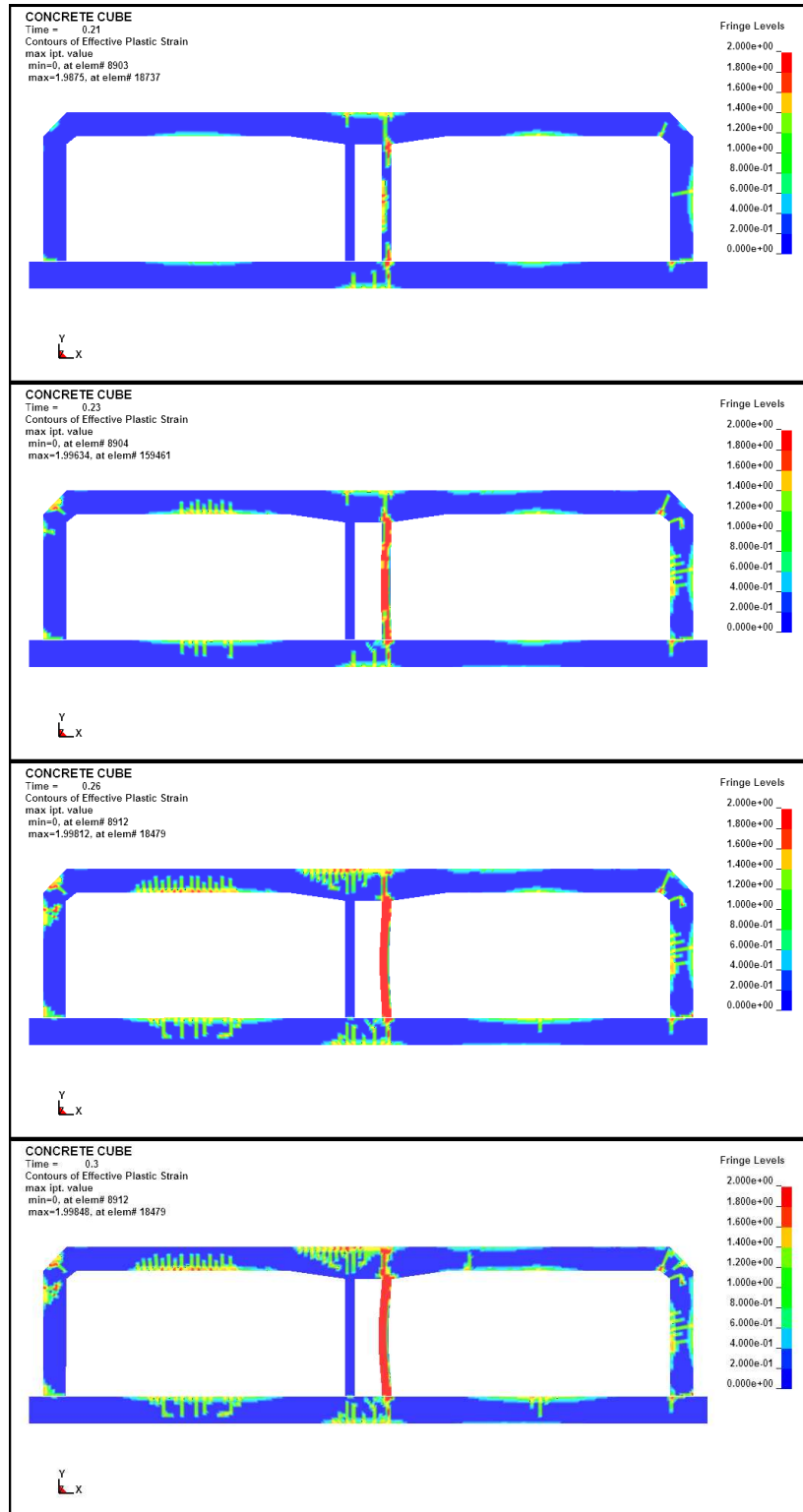


Figure 3.8: Damage plots tunnel in soft soil for a reduced BLEVE

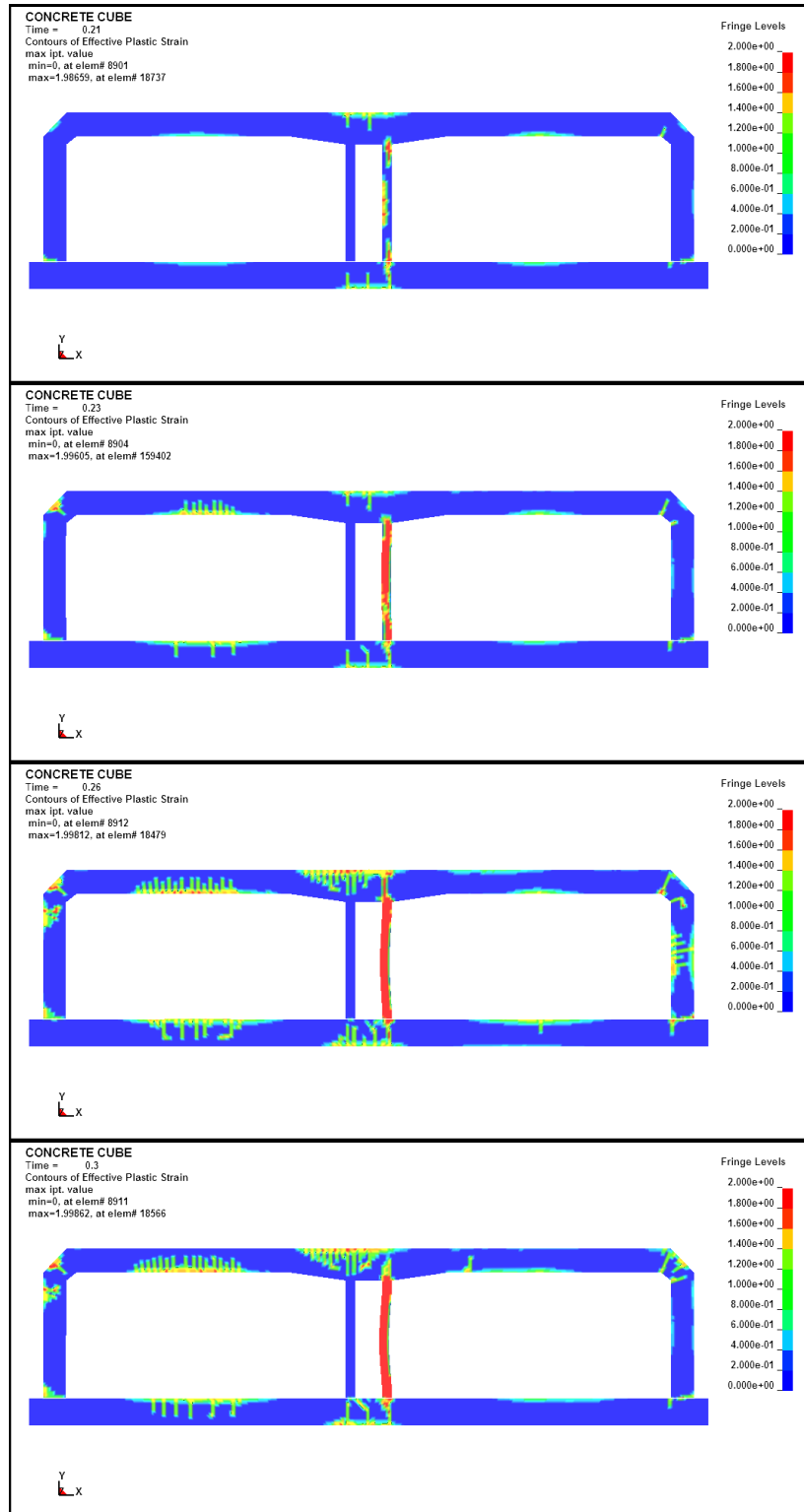


Figure 3.9: Damage plots tunnel in stiff soil for a reduced BLEVE

The concrete strains caused by the permanent load are shown in figure 3.10. The maximum concrete strain in compression is 0,36‰, which is lower than the compressive failure strain of 3,5‰.

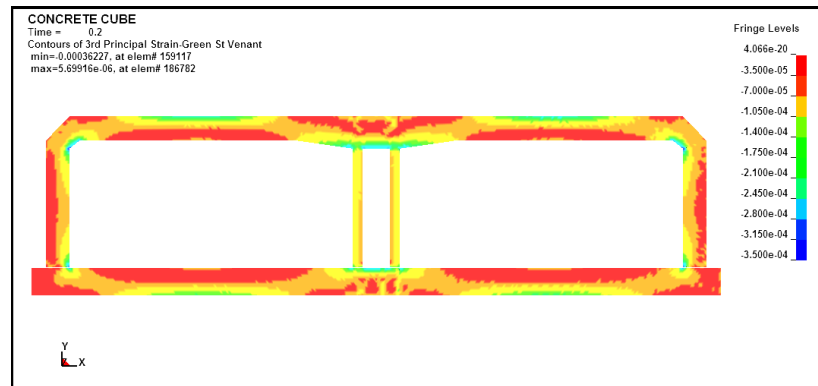


Figure 3.10: Concrete strains due to self-weight and soil and water pressure

The evolution of the concrete strains is shown in figure 3.11 and 3.12 respectively for soft and stiff soil. At $t = 0.23$ sec the concrete failure strain is reached over the full height of the inner wall. The inner wall will collapse.

Observe that the differences between soft soil and stiff soil are small.

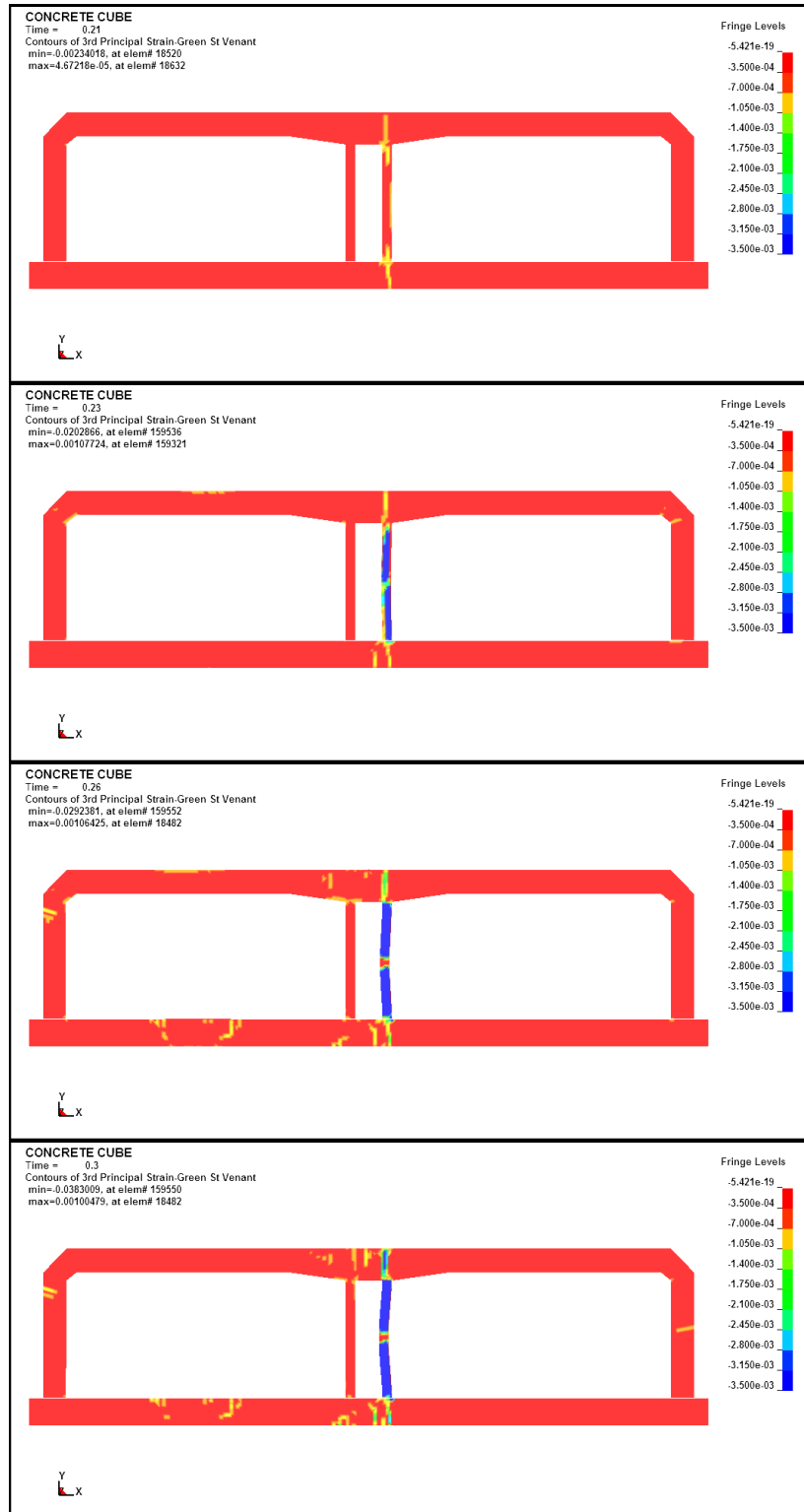


Figure 3.11: Concrete strains tunnel in soft soil for a reduced BLEVE

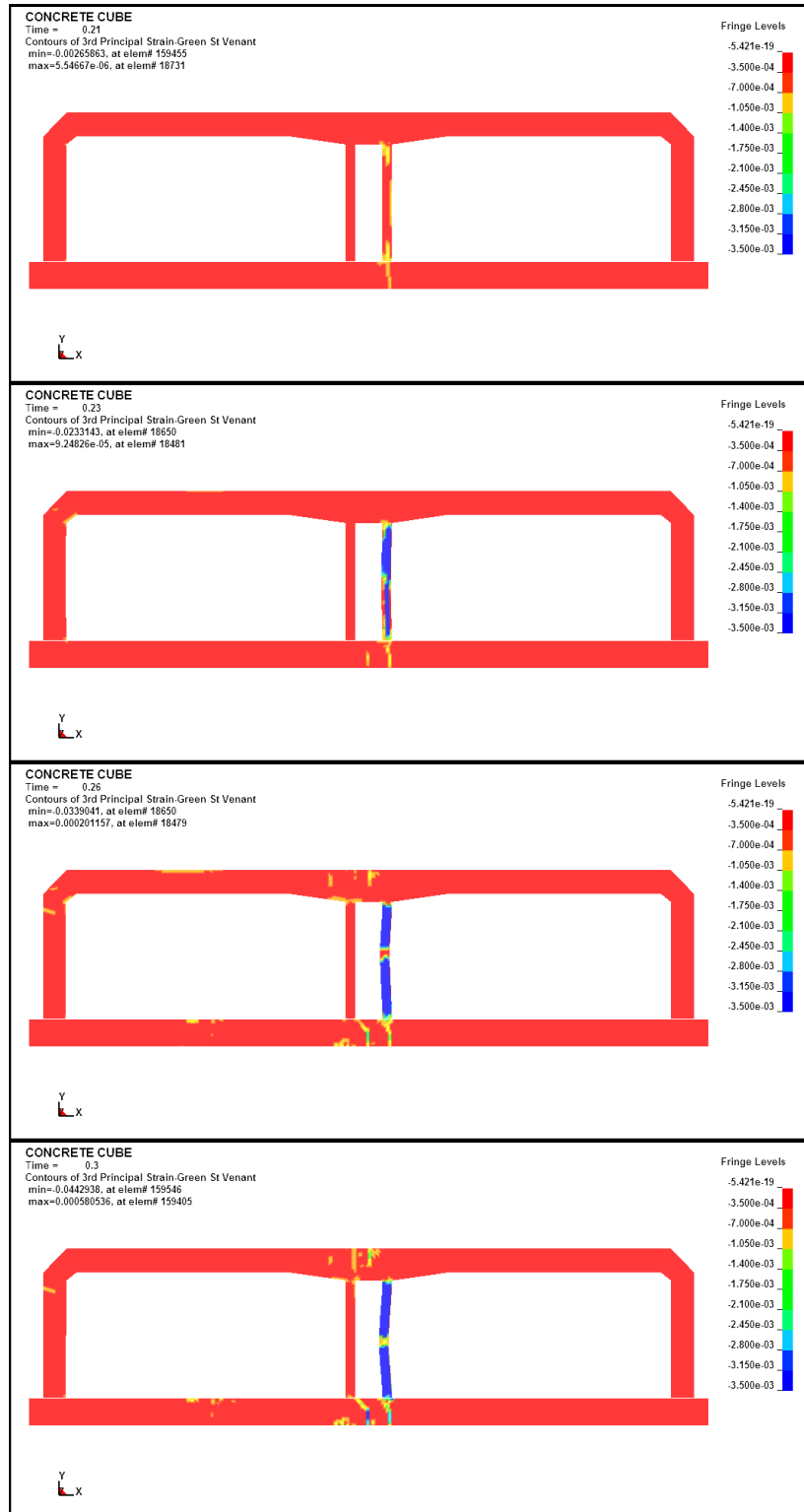


Figure 3.12: Concrete strains tunnel in stiff soil for a reduced BLEVE

3.4 Reinforcement stresses

The reinforcement stresses in the roof and the floor are studied in the elements as indicated in figure 3.13. The reinforcement stresses in the walls are studied in the elements as indicated in figure 3.14.

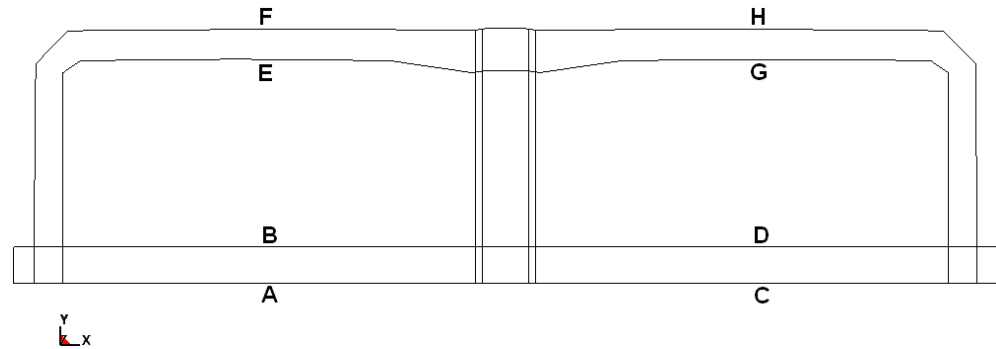


Figure 3.13: Beam elements used for analysing reinforcement stresses in roof and floor

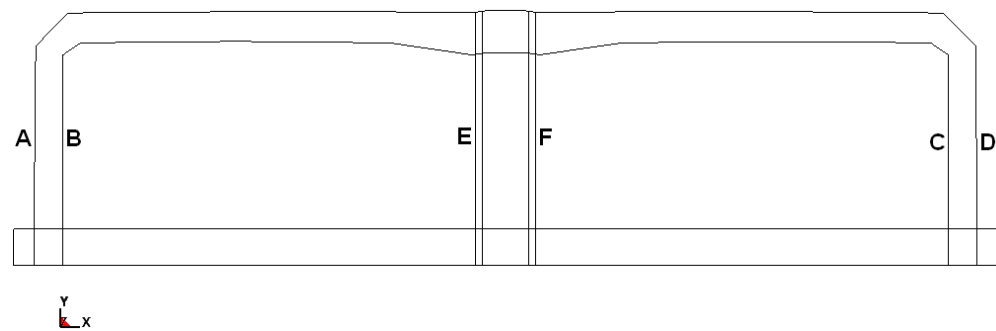


Figure 3.14: Beam elements used for analysing the reinforcement stresses in the walls

Figures 3.15 to 3.18 show the evolution of the reinforcement stresses in the floor, roof and wall reinforcement for soft and stiff soil.

The maximum reinforcement stress in soft soil occurs at the top of the floor of the left tunnel tube and is equal to 155 MPa. The maximum reinforcement stress in stiff soil occurs at the bottom of the roof of the left tunnel tube and is equal to 220 MPa.

For a soft soil the maximum reinforcement stress in the walls occurs in the inner wall and the inside of the outer wall of the right tunnel tube and is equal to 100 MPa. For a stiff soil the maximum reinforcement stress in the walls occurs in the inner wall of the right tunnel tube and is equal to 115 MPa.

Observe that no yielding of the reinforcement occurs.

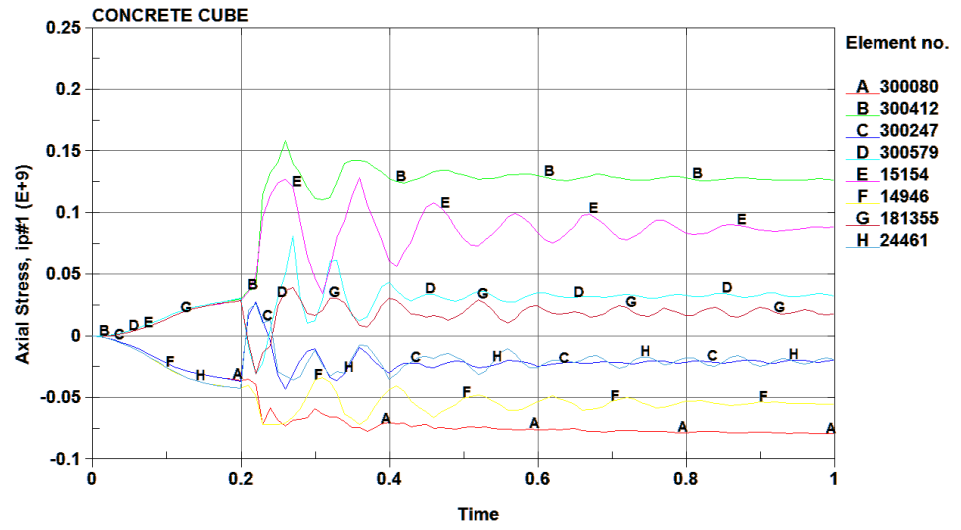


Figure 3.15: Steel stresses in roof and floor reinforcement in soft soil for a reduced BLEVE

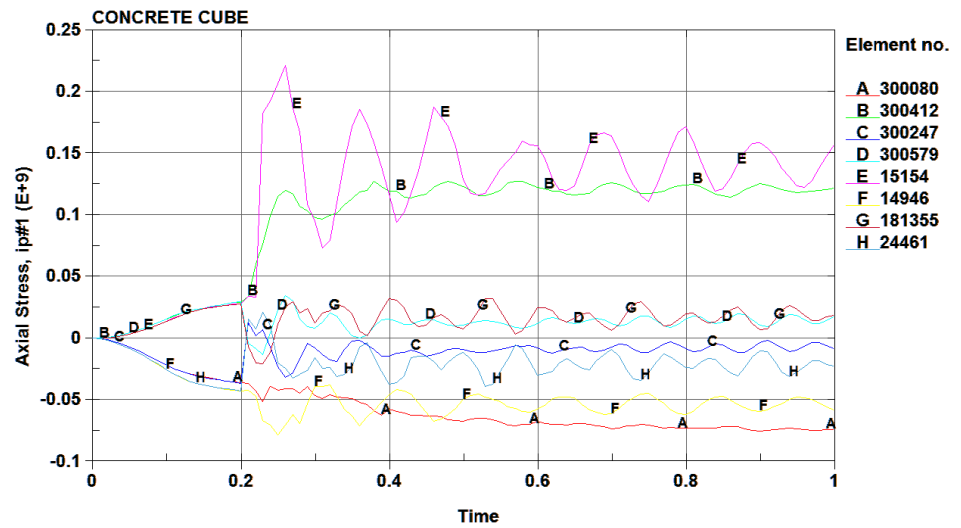


Figure 3.16: Steel stresses in roof and floor reinforcement in stiff soil for a reduced BLEVE

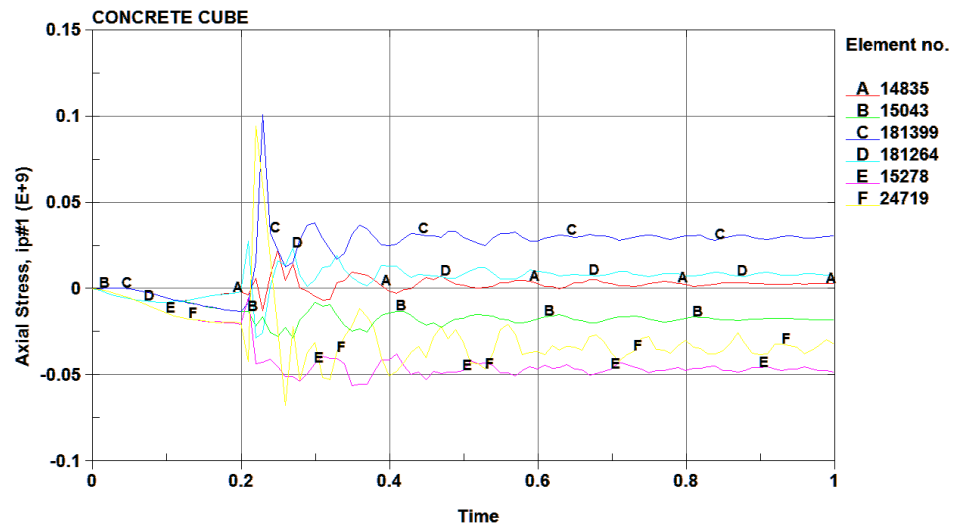


Figure 3.17: Steel stresses in wall reinforcement in soft soil for a reduced BLEVE

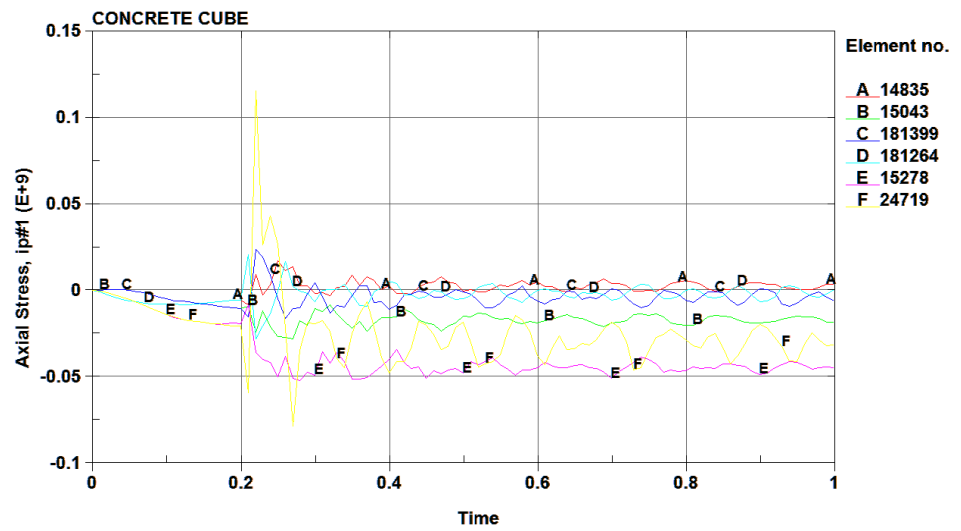


Figure 3.18: Steel stresses in roof and floor reinforcement in stiff soil for a reduced BLEVE

3.5 Soil displacements, displacements, velocities and accelerations

The soil displacements, velocities and accelerations are studied in the nodes as indicated in figure 3.19. The distance between the nodes is 0,25 m. The evolution of the soil displacements, velocities and accelerations is shown in figure 3.20 to 3.22. Because the results for soft and stiff soil are nearly the same, only the results for soft soil are shown.

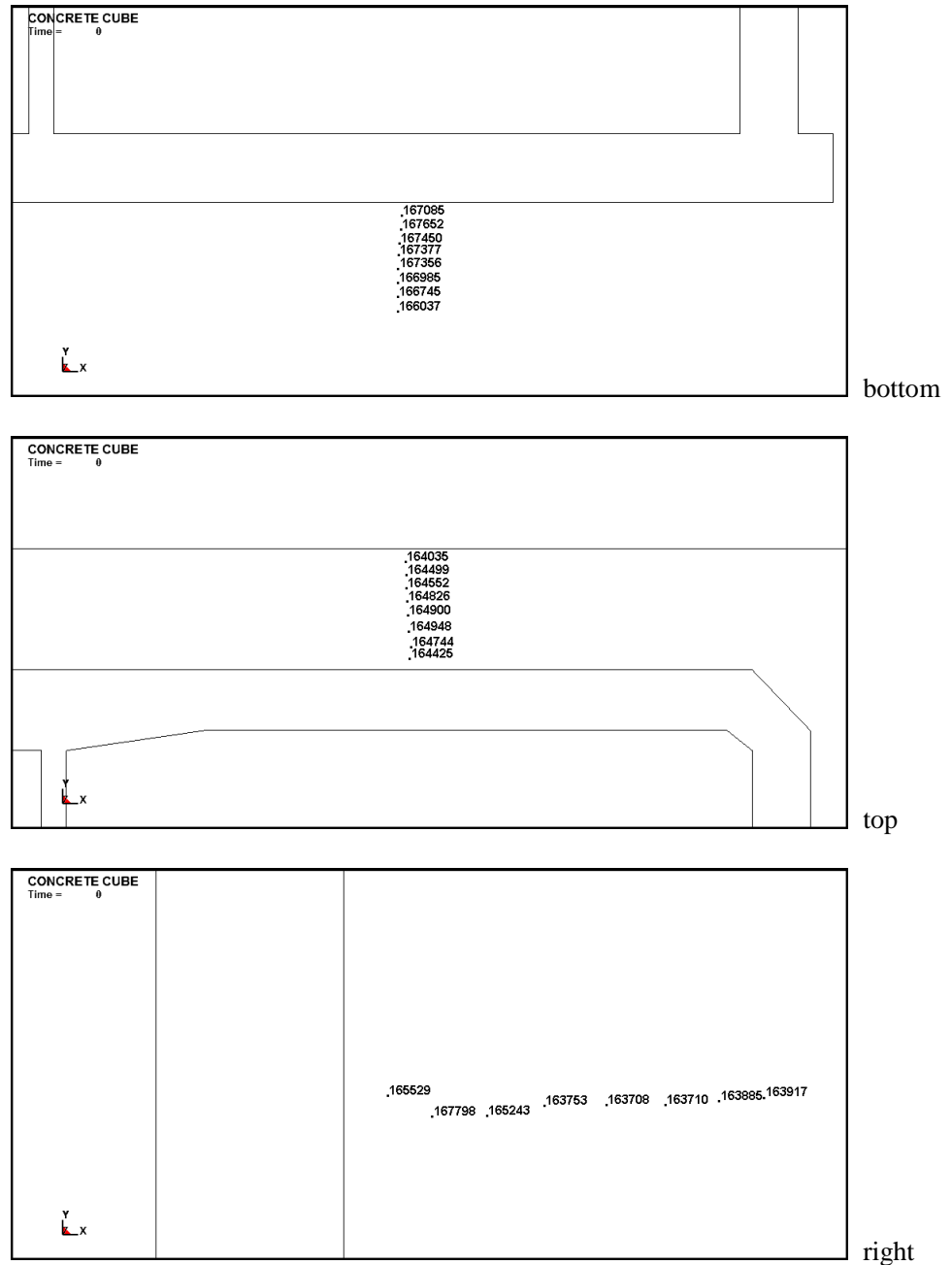


Figure 3.19: Nodes used for analysing the soil displacements, velocities and accelerations

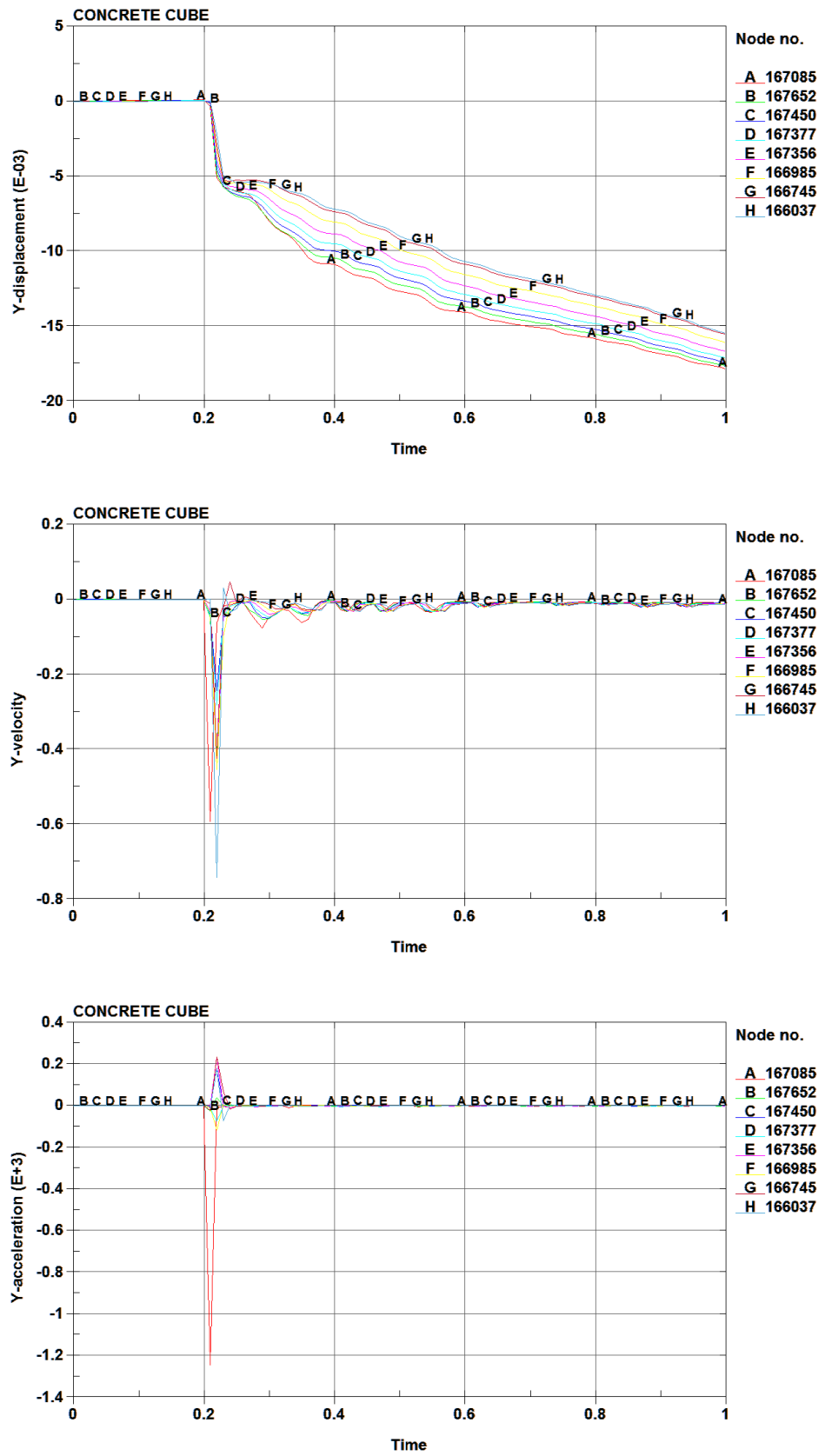


Figure 3.20: Soil displacements, velocities and accelerations beneath the tunnel floor for a reduced BLEVE

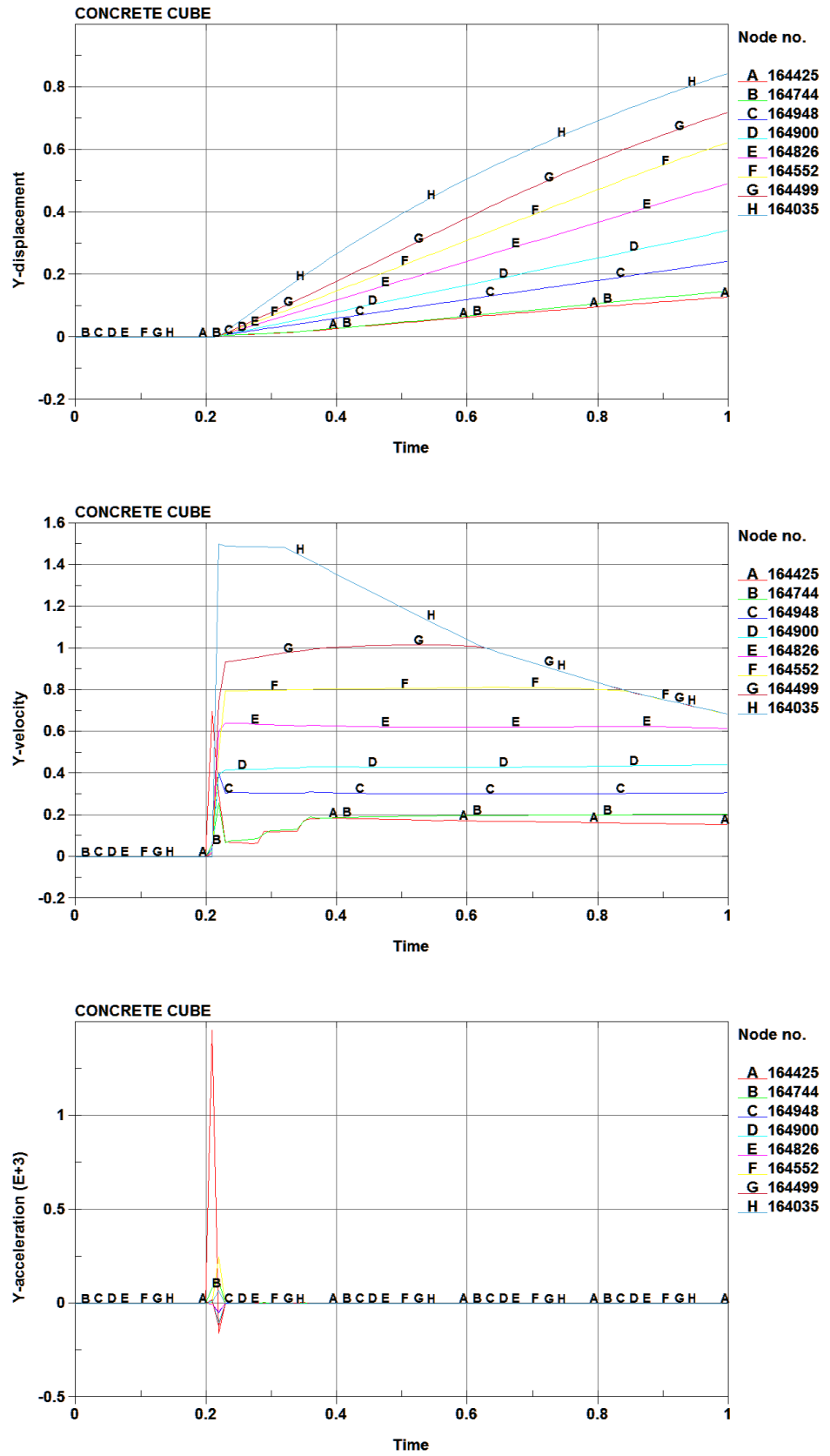


Figure 3.21: Soil displacements, velocities and accelerations above the tunnel roof for a reduced BLEVE

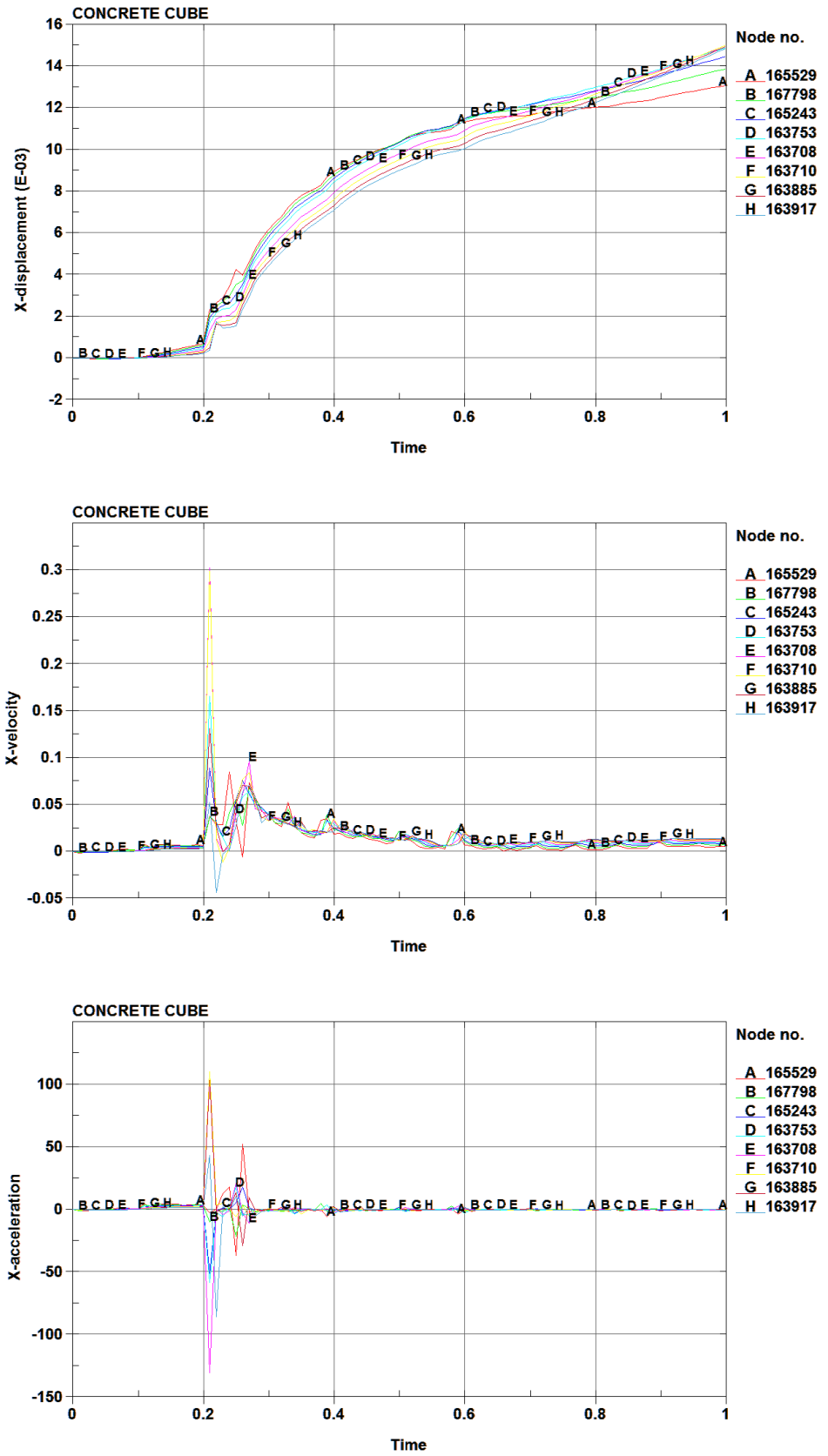


Figure 3.22: Soil displacements, velocities and accelerations next to the outer tunnel wall for a reduced BLEVE

4 Analysis results maximum BLEVE

4.1 Introduction

In this chapter the results of the finite element analyses for the maximum BLEVE-load are presented. First, in section 4.2 the displacements of the tunnel are discussed. In section 4.3 the concrete damage and strains are given. In section 4.4 the reinforcement stresses and strains are presented. Finally, in section 4.5 the soil stresses, displacements, velocities and accelerations are given.

4.2 Tunnel displacements

Figure 3.1 shows the nodes in the roof and floor that have been used for analysing the vertical displacements. Figure 3.2 shows the nodes in the walls that have been used for analysing the horizontal displacements.

The vertical displacement histories of the roof and the floor are presented in figure 4.1 and 4.2 for respectively soft and stiff soil. The horizontal displacement histories of the walls are presented in figure 4.3 and 4.4.

The vertical displacement histories show very large vertical displacements of the roof in both tunnel tubes. These displacements are an order of magnitude larger than the displacements due to a reduced BLEVE-load. The total roof rotates around the inner walls. The roof in the right tunnel tube moves in 1 sec almost 2,5 m upward. Such large displacements lead to mistrust of the results of the calculations. Normally, in such a situation is a collapse occurred and/ or secondary effects play a significant role. For this reason it can be stated that the roof of each tube collapses under the influence of a maximum BLEVE-load.

Similar with the response to a reduced BLEVE-load, the inner wall of the right tunnel tube will move in direction of the escape tube. The maximum horizontal displacement of this wall is 0,5 m. From 0.3 sec after application of the explosion, the remaining walls deform substantially.

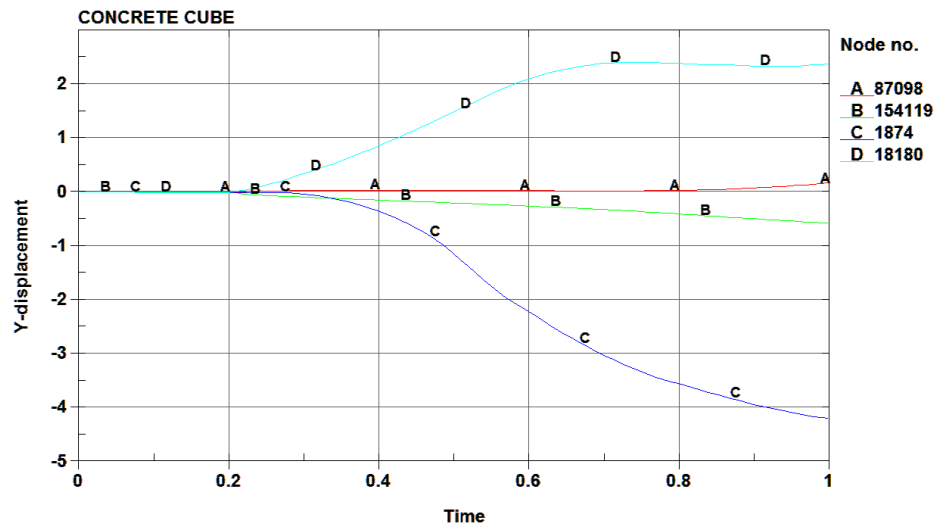


Figure 4.1: Vertical displacements of roof and floor in soft soil for a maximum BLEVE

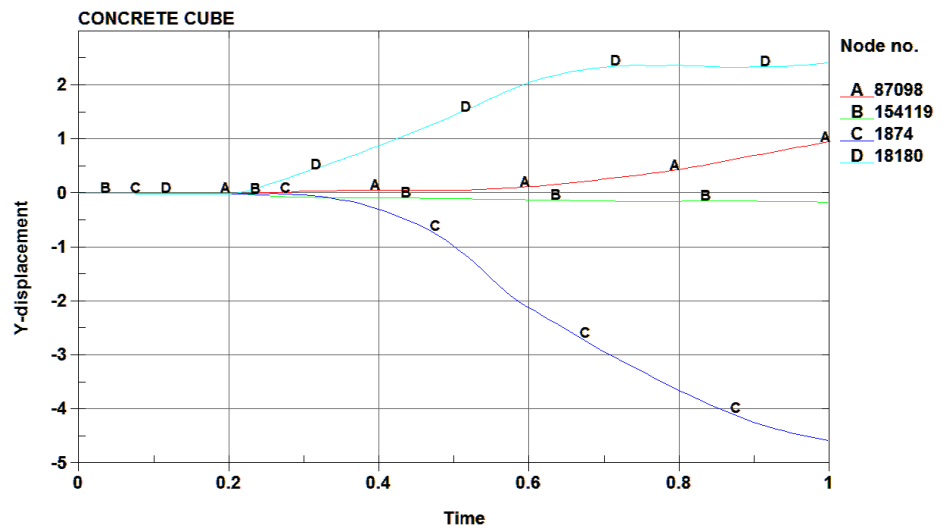


Figure 4.2: Vertical displacements of roof and floor in stiff soil for a maximum BLEVE

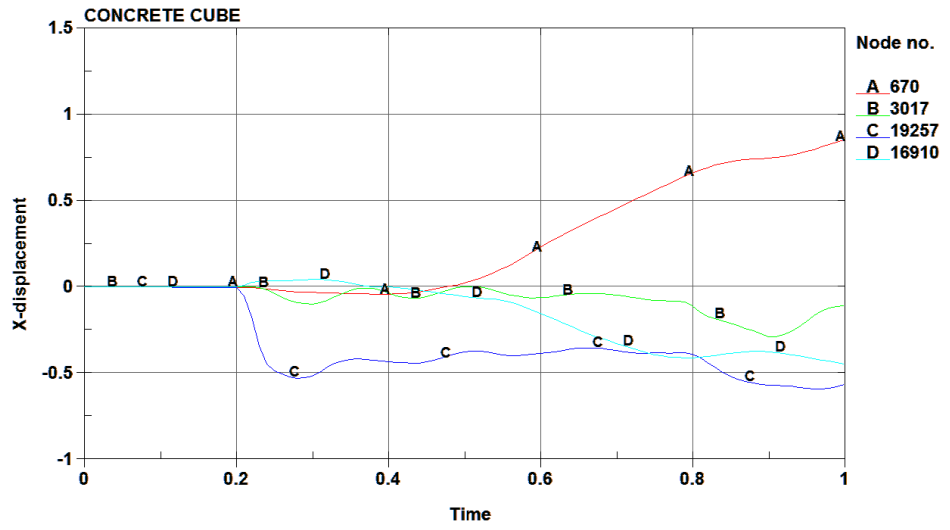


Figure 4.3: Horizontal displacements of walls in soft soil for a maximum BLEVE

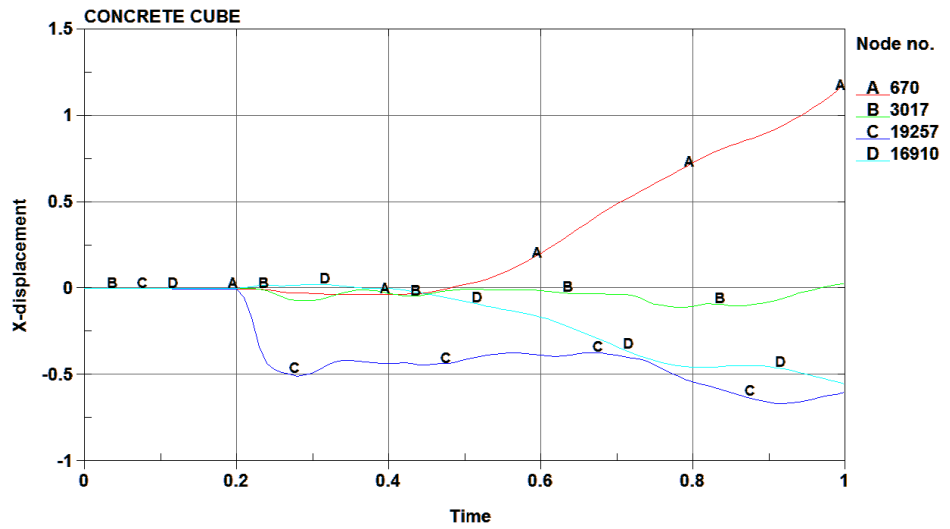


Figure 4.4: Horizontal displacements of walls in stiff soil for a maximum BLEVE

4.3 Concrete damage and strains

The evolution of the damage is shown in figure 4.5 and 4.6 respectively for soft and stiff soil.

The inner wall is completely damaged after 0,01 sec of blast load. Because the blast load is still present then, there's a possibility that parts of this wall will hit the other inner wall, which may lead to failure of the other inner wall too. The finite element analyses don't account for this phenomenon.

At $t = 0,3$ sec the roof is fully damaged. Based on the large deformations and the considerable amount of damage, it is very likely that the tunnel structure will collapse under the influence of a maximum BLEVE-load.

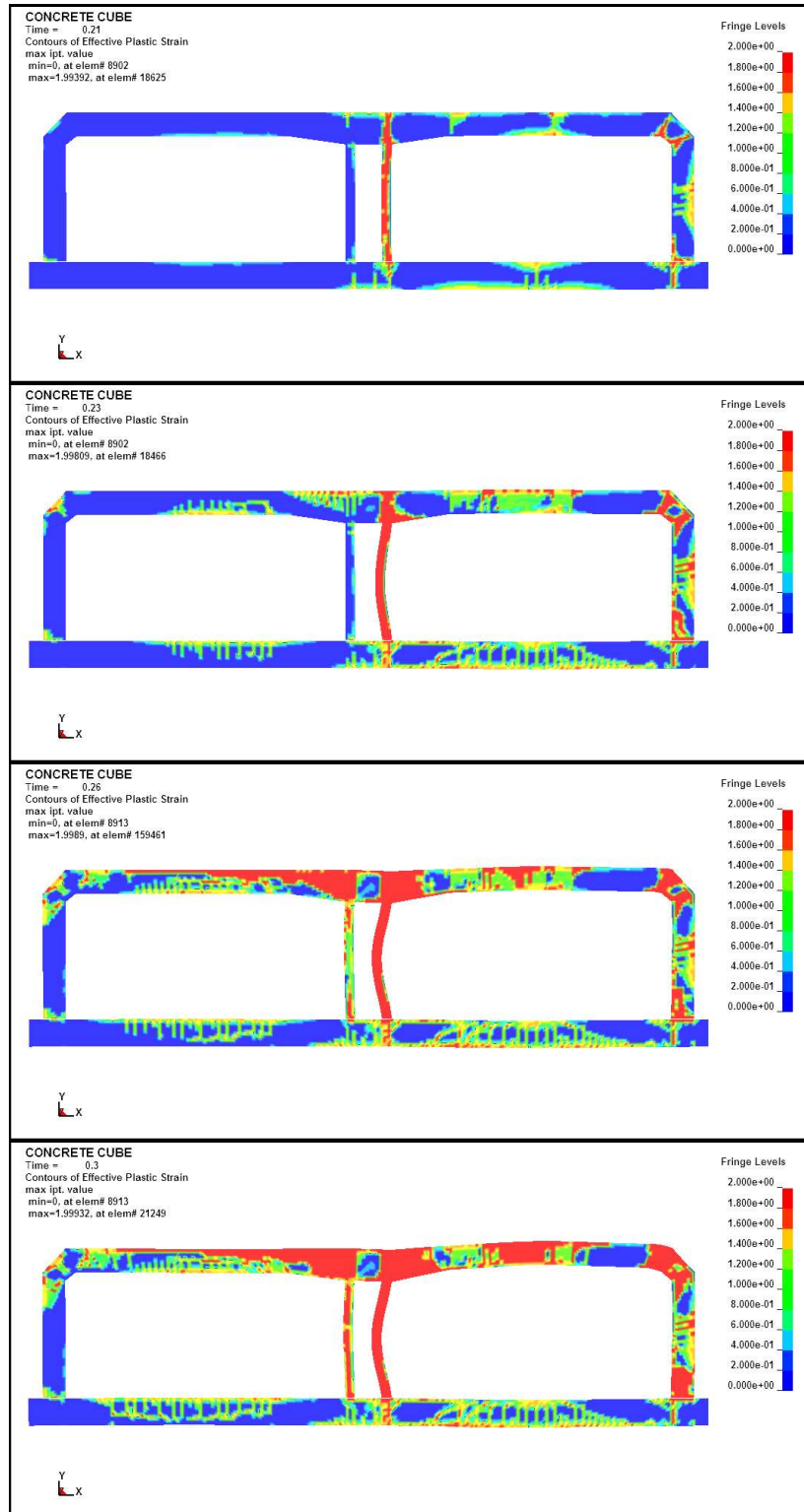


Figure 4.5: Damage plots tunnel in soft soil for a maximum BLEVE

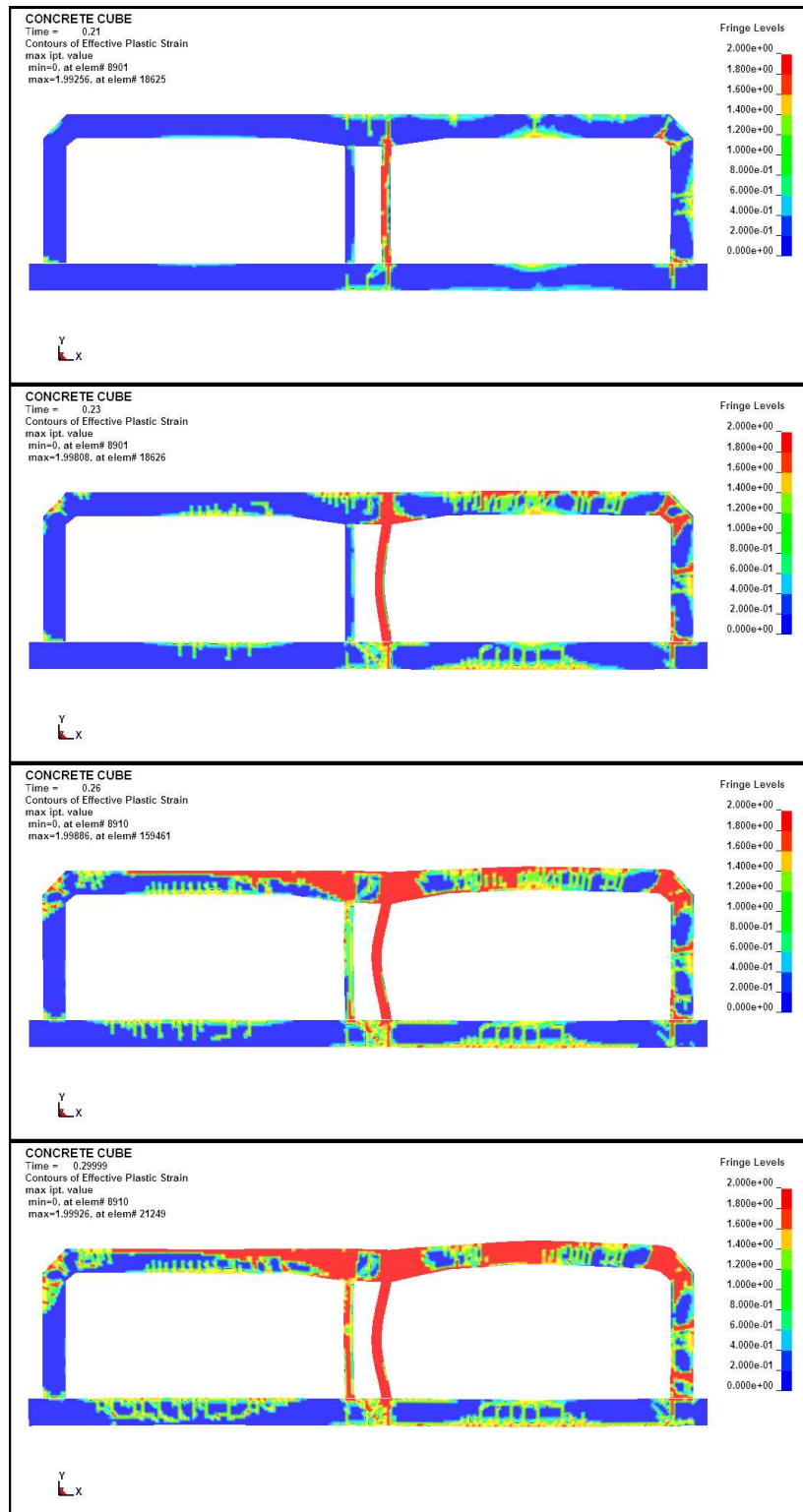


Figure 4.6: Damage plots tunnel in stiff soil for a maximum BLEVE

The evolution of the concrete strains is shown in figure 4.7 and 4.8 respectively for soft and stiff soil. Already at $t = 0.21$ sec the concrete failure strain is reached over the full height of the inner wall. The inner wall will fail. Observe that the differences between soft soil and stiff soil are small.

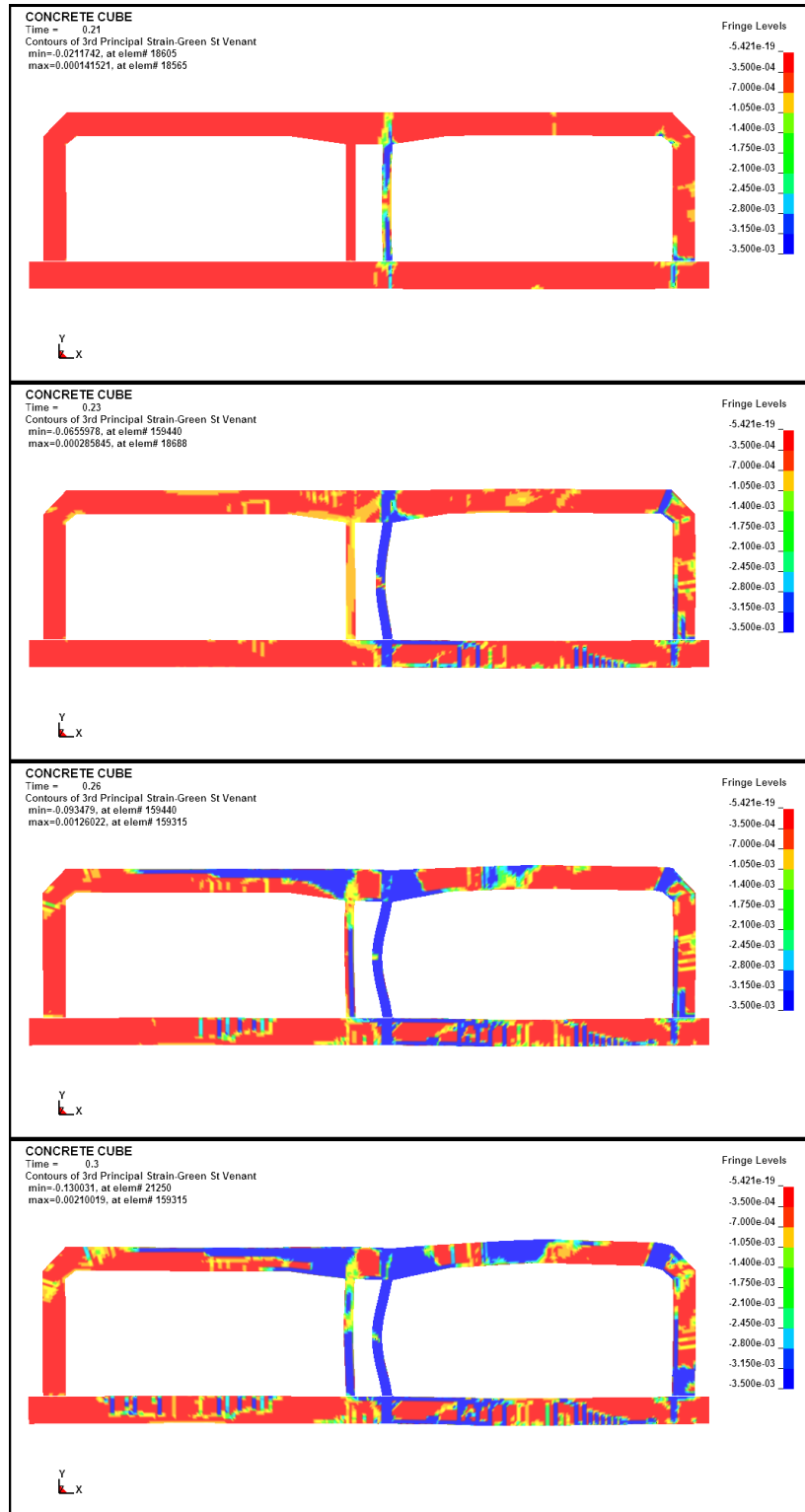


Figure 4.7: Concrete strains tunnel in soft soil for a maximum BLEVE

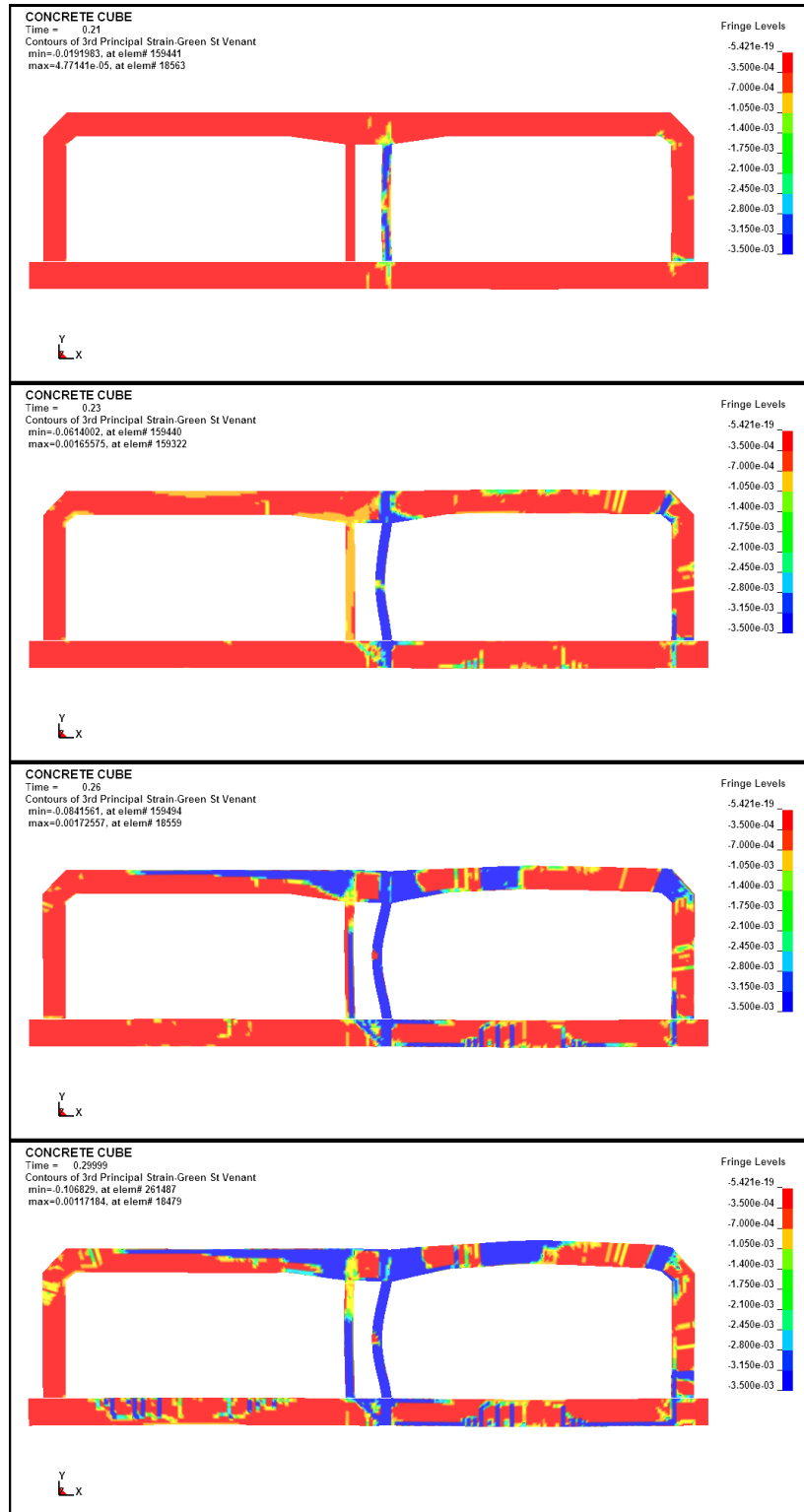


Figure 4.8: Concrete strains tunnel in stiff soil for a maximum BLEVE

4.4 Reinforcement stresses and strains

The reinforcement stresses are studied in the elements as indicated in figure 3.13 and 3.14. Figures 4.9 to 4.12 show the evolution of the reinforcement stresses in the floor, roof and wall reinforcement for soft and stiff soil.

The maximum reinforcement stress in soft and stiff soil occurs at the top of the roof of the left tunnel tube and exceeds the yield strength of 500 MPa. The maximum reinforcement stress in the walls occurs at the outside of the outer wall of the left tunnel tube and exceeds the yield strength.

Figures 4.13 to 4.16 show the evolution of the plastic strain in the reinforcement. The maximum strain in the reinforcement is located at the top of the roof of the right tunnel tube and is about 8%. Considering a failure strain between 7% and 10% (with a design value of the failure strain of 3,5%), there's a possibility that the reinforcement at the top of the roof of the right tunnel tube will break.

As noted earlier, based on the large deformations, the considerable amount of damage, the excess of the failure strain of the concrete and exceeding the yield stress of the reinforcement, it is very likely that the tunnel construction will collapse under the influence of a maximum BLEVE-load.

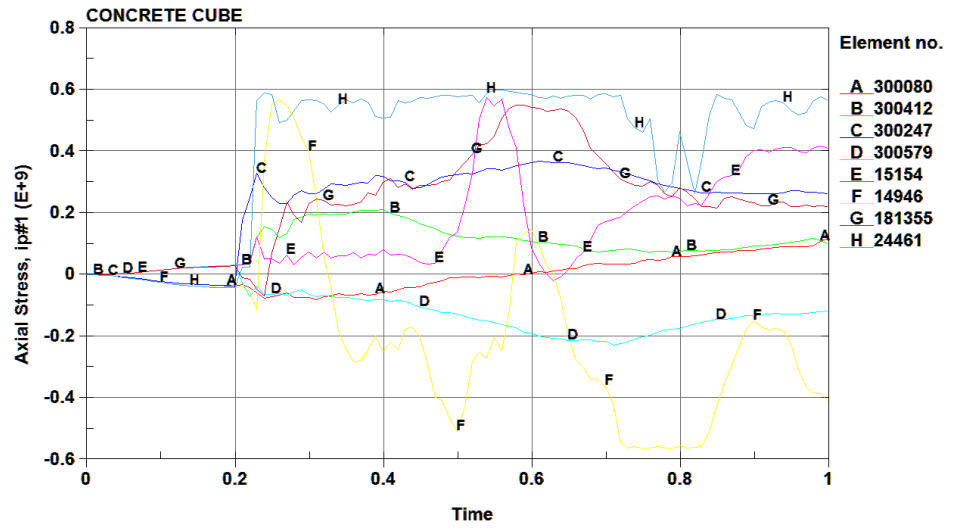


Figure 4.9: Steel stresses in roof and floor reinforcement in soft soil for a maximum BLEVE

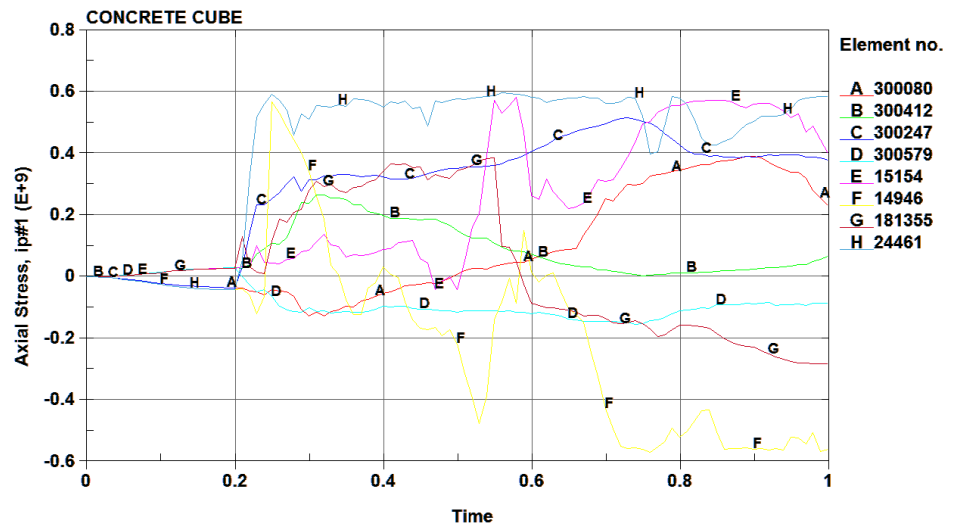


Figure 4.10: Steel stresses in roof and floor reinforcement in stiff soil for a maximum BLEVE

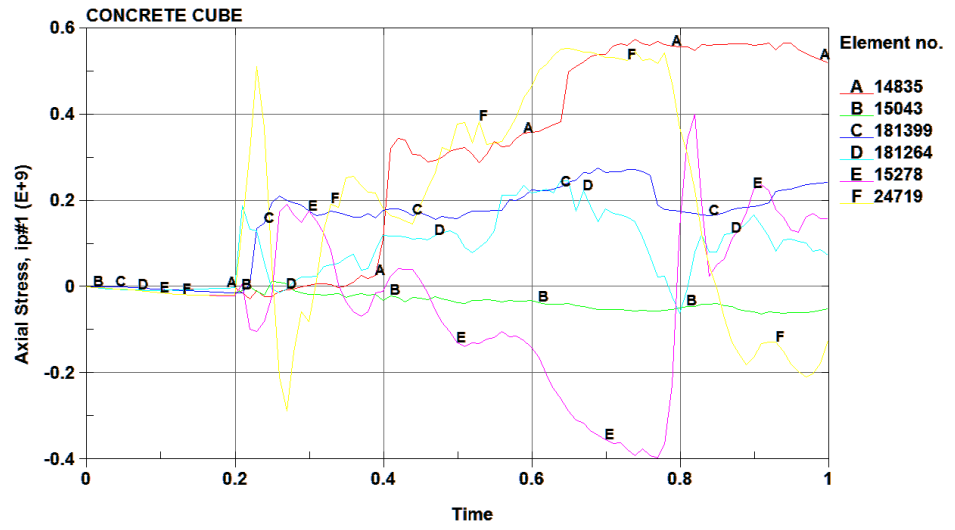


Figure 4.11: Steel stresses in wall reinforcement in soft soil for a maximum BLEVE

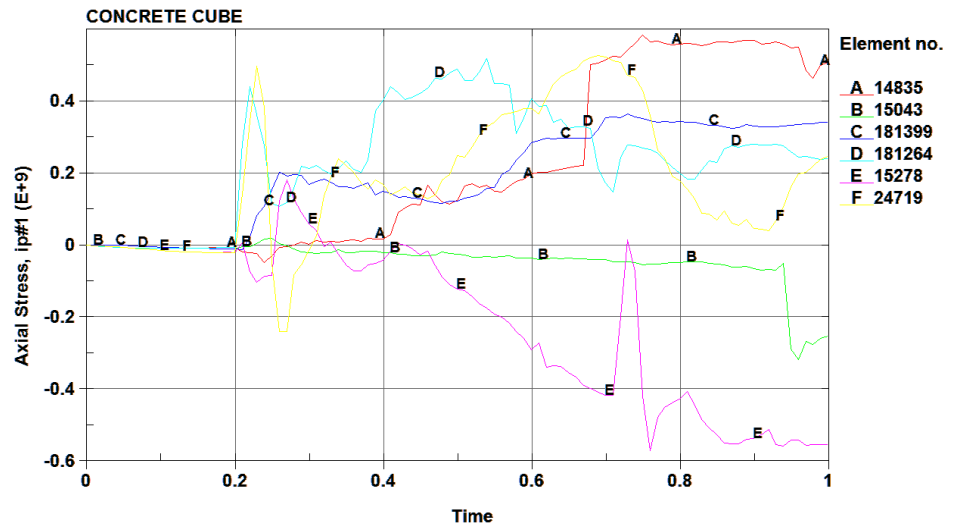


Figure 4.12: Steel stresses in wall reinforcement in stiff soil for a maximum BLEVE

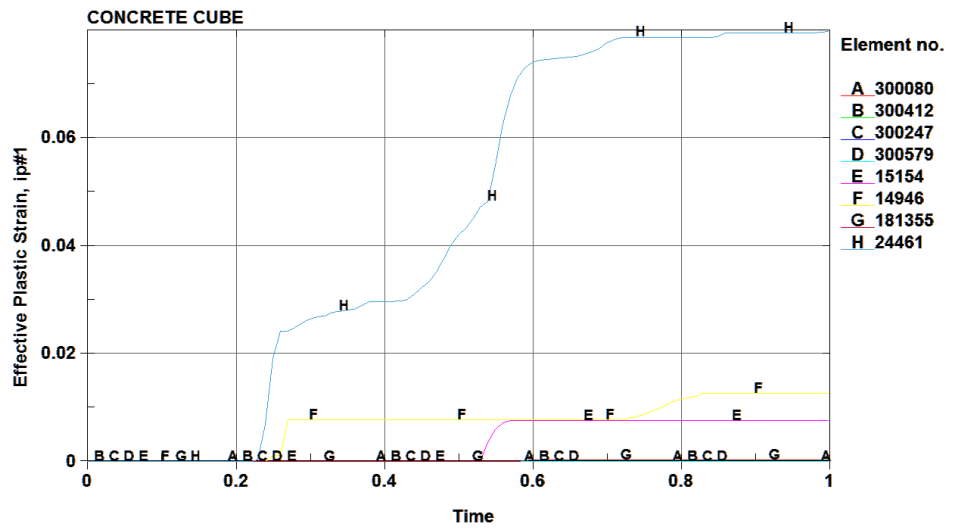


Figure 4.13: Plastic strain in roof and floor reinforcement in soft soil for a maximum BLEVE

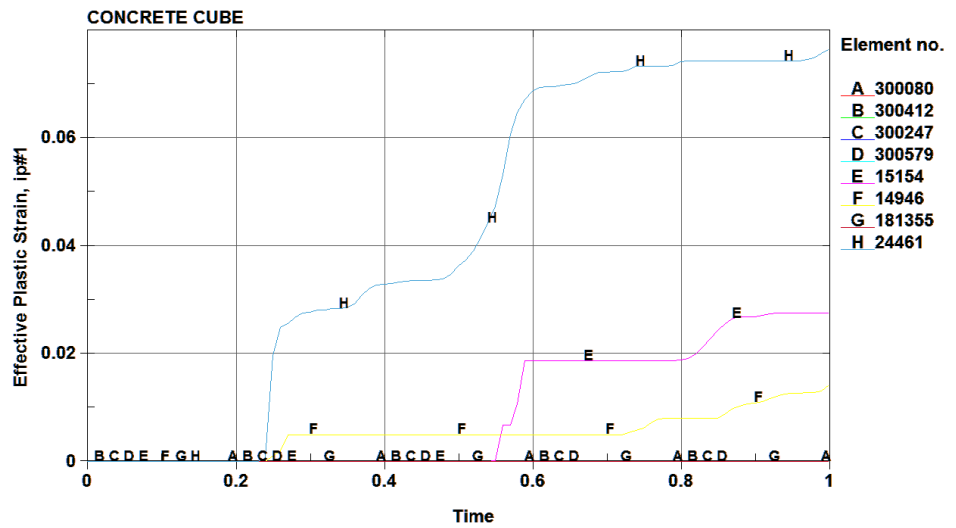


Figure 4.14: Plastic strain in roof and floor reinforcement in stiff soil for a maximum BLEVE

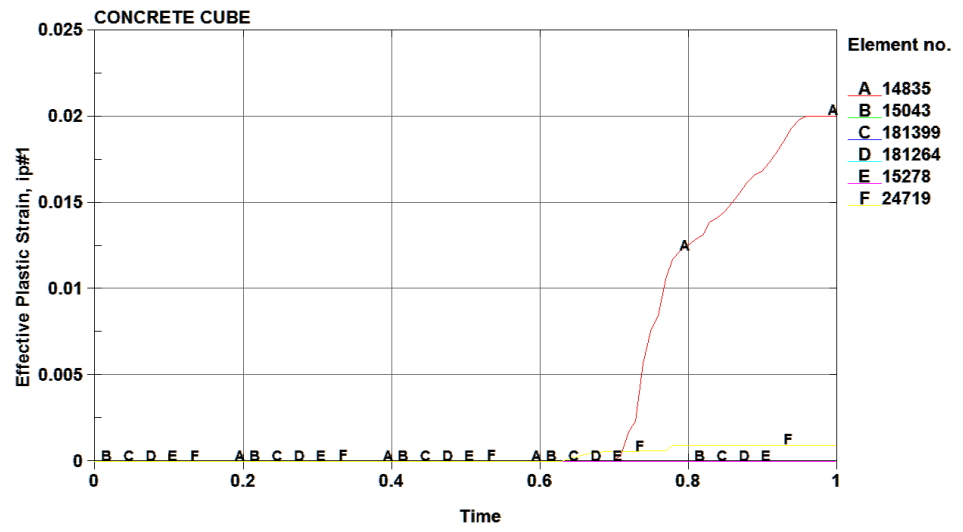


Figure 4.15: Plastic strain in wall reinforcement in soft soil for a maximum BLEVE

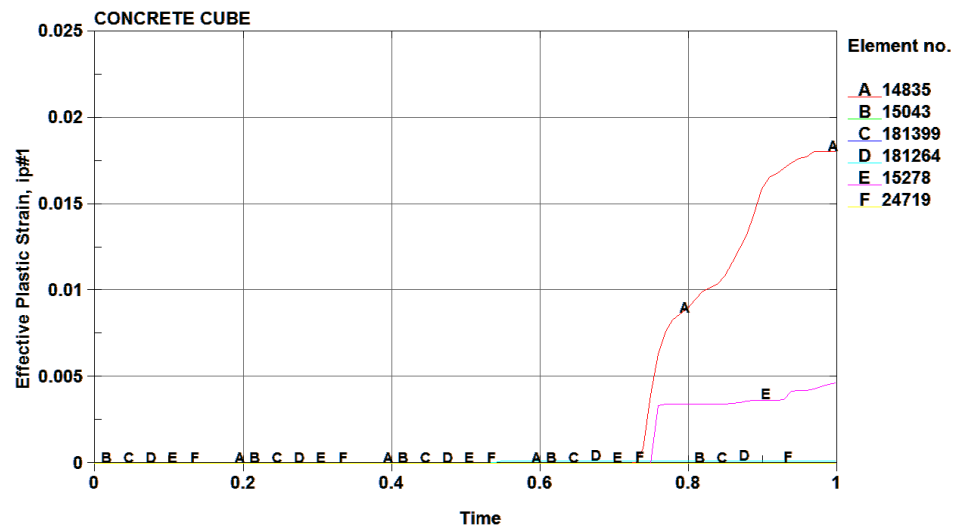


Figure 4.16: Plastic strain in wall reinforcement in stiff soil for a maximum BLEVE

4.5 Soil displacements, displacements, velocities and accelerations

The soil displacements, velocities and accelerations are studied in the nodes as indicated in figure 3.19. The distance between the nodes is 0,25 m. The evolution of the soil displacements, velocities and accelerations is shown in figure 4.17 to 4.19. Because the results for soft and stiff soil are nearly the same, only the results for soft soil are shown.

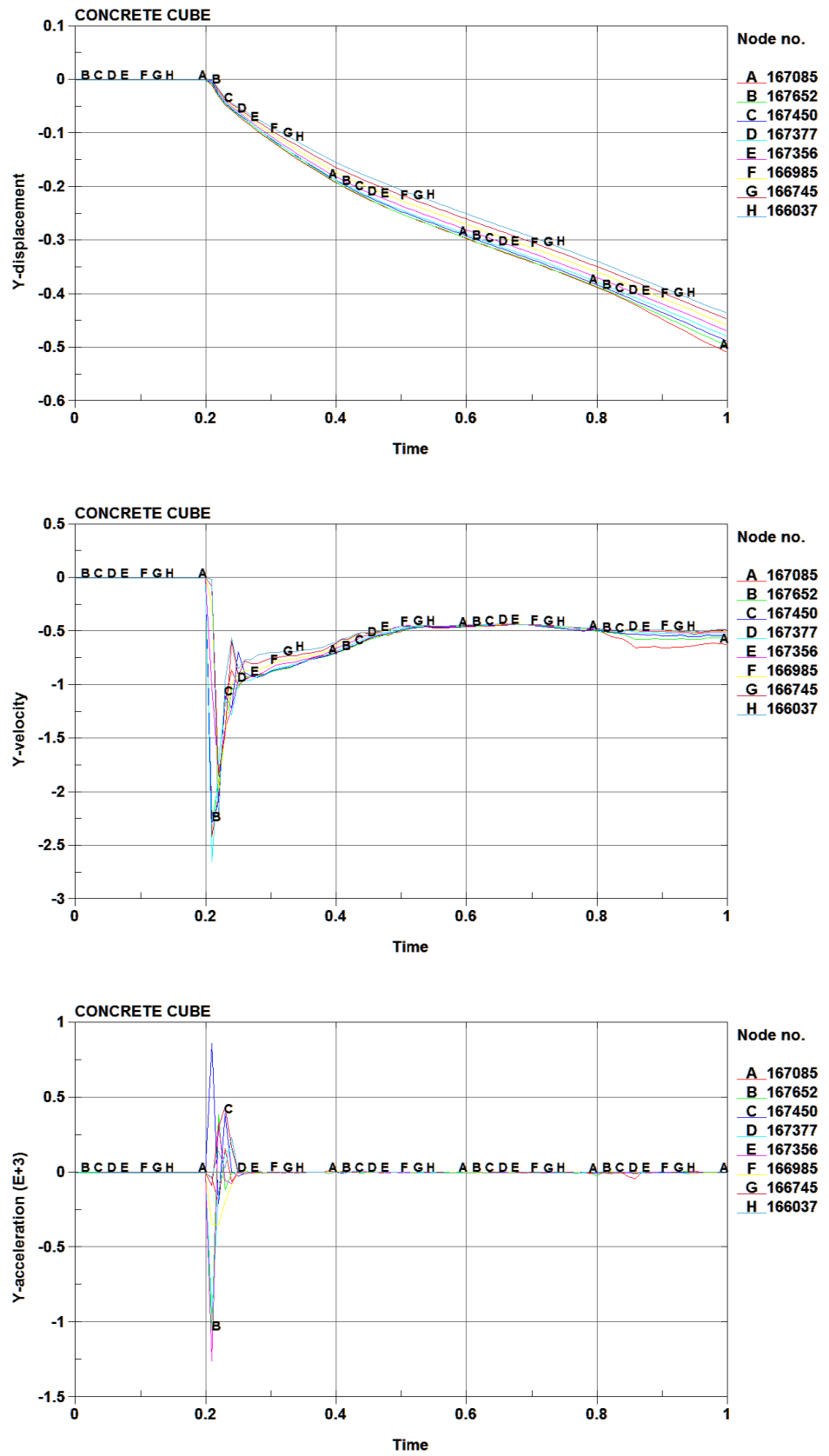


Figure 4.17: Soil displacements, velocities and accelerations beneath the tunnel floor for a maximum BLEVE

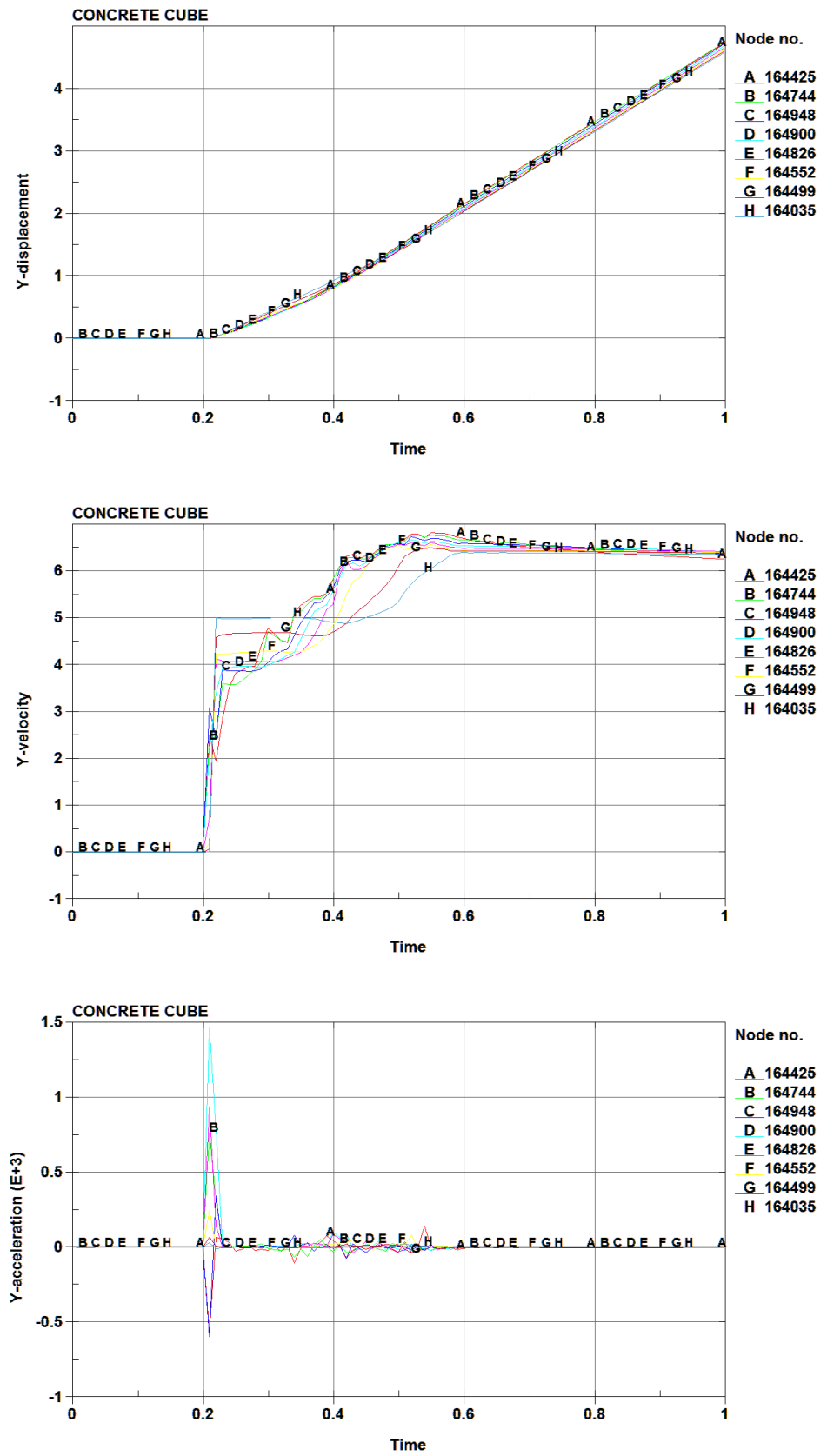


Figure 4.18: Soil displacements, velocities and accelerations above the tunnel roof for a maximum BLEVE

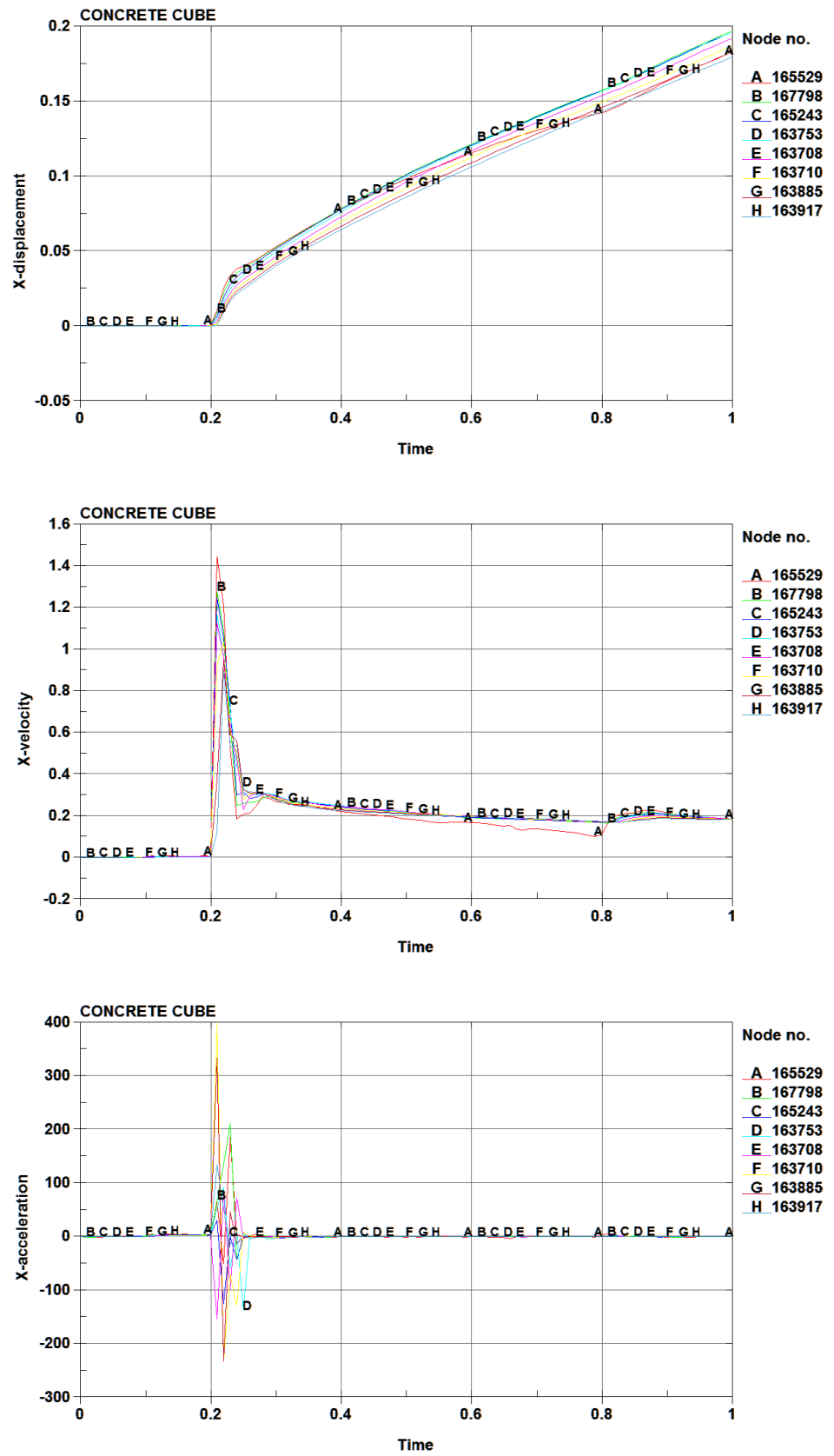


Figure 4.19: Soil displacements, velocities and accelerations next to the outer tunnel wall for a maximum BLEVE

5 Comparison results LS-DYNA and PLAXIS

The results of the LS-DYNA and the PLAXIS calculations show some differences. For instance the upward displacement of the roof due to a reduced BLEVE-load is approximately 10 mm in the LS-DYNA calculation and about four times larger in the PLAXIS calculation.

The differences between the results of the calculations in LS-DYNA and PLAXIS can be explained by the following aspects:

1. Concrete model
 - a. LS-DYNA: damage model with strain rate hardening
 - b. PLAXIS: elasto-plastic model
2. Soil model
 - a. LS-DYNA: Mohr-Coulomb model (1-phase)
 - b. PLAXIS: hardening soil model (2-phase)
3. Water level
 - a. LS-DYNA: 11 m above tunnel
 - b. PLAXIS: 2 m above tunnel
4. Mesh size tunnel
 - a. LS-DYNA: 12 elements over roof height
 - b. PLAXIS: 1 element over roof height

The effect of the differences in material models, water level and mesh size on the results remains questionable. Further research is necessary, especially for a better understanding of the soil behaviour.

6 Conclusions and recommendations

From the present study the following conclusions can be drawn:

1. A reduced BLEVE-load ($\Delta p = 510$ kPa, $I = 12$ kPa·s) leads to local failure:
 - a. The inner wall of the tunnel tube, where the explosion takes place, will collapse within 0.03 sec;
 - b. Cracking occurs at the inside of the roof, floor and walls;
 - c. Cracking occurs at the outside of the roof and floor (at the connection between the walls and at the connection between the roof and the outside walls).
2. A maximum BLEVE-load ($\Delta p = 1600$ kPa, $I = 64$ kPa·s) leads to overall failure:
 - a. The inner wall of the tunnel tube, where the explosion takes place, will collapse within 0.01 sec;
 - b. Yield and possible fracture of the reinforcement lead to large deformations.

The differences in the dynamic behaviour of a tunnel in soft soil and a tunnel in stiff soil are small. The differences are mainly visible in the crack pattern. A soft soil gives more cracks in the tunnel lining than a stiff soil. The differences in results between soft and stiff soil are limited and do not affect the conclusions above.

The results of the calculations in LS-DYNA and PLAXIS show some differences. For example, the upward displacement of the roof caused by a BLEVE-II load is 10 mm in LS-DYNA. The upward displacement in PLAXIS is about four times larger. The differences are particularly caused by defects in the material model for concrete in PLAXIS (especially in the non-linear). To a lesser extent, also modelling aspects (e.g. element size) play a role.

The calculations have shown that a prediction can be given of the dynamic behaviour of a tunnel under impact load. The results show that the behaviour is dominated by the tunnel structure. Therefore, in designing BLEVE-resistant tunnels there is a need for an advanced material model for the tunnel lining. The surrounding soil must be included in the model, however, within the prescribed limits, the soil properties are not important. A simple material model for the surrounding soil is sufficient in this case. The reliability of the material models for concrete under dynamic conditions is not validated in the present study. An experimental validation is required.

References

- [1] A.H.J.M. Vervuurt, et al., Effect of explosions in tunnels. Preliminary assessment of the structural response, TNO-report 2007-D-R0156, Delft, 2007
- [2] J. Mediavilla, et al., Blast response of the Calland tunnel with LS-DYNA: a comparative study, TNO-report 2008-D-R0223/B, Rijswijk, 2008
- [3] M. Xie, D. Roekaerts, On the need for experimental data sets for BLEVE model validation, Report TU Delft / DC/COB "L1", Delft, 2009